Analysis of Diversity Techniques for Improving
the Performance of DS-CDMA Data Networks

By

Richard S. C. Wong
B. Eng., University of Victoria, 1995

A Thesis Submitted in Partial Fulfillment of the
Requirements for the Degree of

MASTER OF APPLIED SCIENCE

In the Department of Electrical and Computer Engineering

We accept this thesis as conforming
to the required standard

[redacted]

Dr. Vijay K. Bhargava, Supervisor (Department of Electrical and Computer Engineering)

[redacted]

Dr. W. S. Lu, Departmental Member (Dept. of Electrical and Computer Engineering)

[redacted]

Dr. X. Li, Outside Member, (Department of Mechanical Engineering)

[redacted]

Dr. F. Santucci, External Examiner

Supervisor: Dr. Vijay K. Bhargava

Abstract

This dissertation investigates two types of diversity techniques for use in direct sequence code division multiple access wireless communication networks. The first diversity system examined is the maximal-ratio combiner (MRC). Two variations of the MRC are compared over a generalized fading channel. The results reveal that the pre-selection MRC outperforms finite tap decisions MRC. The combination of a strong specular component and a heavily decayed multipath intensity profile may result in only a minimal degradation of the receiver performance for a finite tap decisions MRC, and pre-selection MRC over the optimal MRC. Time diversity is the second technique examined. Both Poisson and self-similar traffic models are examined for packet data transmission. The results show that the self-similar traffic has a higher normalized throughput than the Poisson traffic. Also, with a reduced number of fingers in the rake receiver, the performance reduction of the systems with a flatter MIP is higher than that of a more steeply decaying MIP.

Examiners:

[redacted]

Dr. Vijay K. Bhargava, Supervisor (Department of Electrical and Computer Engineering)

[redacted]

Dr. W. S. Lu, Departmental Member (Dept. of Electrical and Computer Engineering)

[redacted]

Dr. X. Li, Outside Member, (Department of Mechanical Engineering)

[redacted]

Dr. F. Santucci, External Examiner (U. of L'Aquila, Dept. of Electrical Engineering)

Table of contents

List of Figures

List of Tables

Acknowledgments

I would like to take this opportunity to express my thanks to all of those people who have helped me throughout my academic career. I would first like to acknowledge my supervisor, mentor, and friend, Dr. Vijay K. Bhargava. Without his guidance and support, my graduate studies would not have been as enjoyable and productive as they have been. I would also like to thank Dr. Qiang Wang for introducing me to research work.

For the last three years I have been part of a very unique research group. The symbiotic relationships that occur there are a great assistance to all that have had the privilege of being a part of the group. I count myself as being very fortunate to have benefited from such an environment. To that end I would like to thank all of the members of the Digital Communications Laboratory. You have provided me with invaluable advice, guidance, and insight. In particular, I would like to thank Mr. Annamalai Annamalai jr. for his collaborations with me. My time with him has been very fruitful and much of the work in this dissertation was a result of my collaboration with him. I am also grateful to Mr. Alex Bhargava for proof-reading this dissertation.

Finally, I would like to thank my family. Their support, encouragement, and patience has allowed me to pursue all of my dreams.

To my family: for their support, encouragement, and understanding.

List of acronyms

ΔB_c	Coherence Bandwidth
Δt_c	Coherence Time
AWGN	Additive white Gaussian noise
CDMA	Code division multiple access
DS-CDMA	Direct sequence CDMA
fBm	fractional Brownian motion
fBn	fractional Brownian noise
FCC	Federal Communications Commission
FDMA	Frequency division multiple access
FEC	Forward Error Correction
FTP	File Transfer Protocol
ISM	Instrumentation, Scientific and Medical
L-MRC	L tap maximal ratio combining
M-MRC	reduced complexity M tap maximal ratio combining
M-SCMRC	M tap selection combining maximal ratio combining
MIP	Multipath intensity profile
MRC	Maximal-ratio combining
PCS	Personal Communications Services
PDF	probability density function
R_{av}	Average number of transmissions
TDMA	Time division multiple access

Chapter 1 Introduction

It has been said that we are undergoing a digital revolution. Much like the industrial revolution, the digital revolution has changed the way we live and cwhat we thought was possible. Personal wireless communications is one of the remaining challenges that remains to be conquered in the digital revolution. Technology is still striving to meet the consumer demand of communications anywhere, at anytime. In this light, the efficient transmission of digital data, and especially digital data packets, has become very important. With the explosion in the popularity of the internet, the demand for wireless packet data services has already arrived and should continue to grow. The challenge of technology is to provide the wireless services that will be an important part of the infrastructure of the digital revolution.

Today, most modern wireless communication systems employ some form or combination of time, frequency, or code division multiple access (TDMA, FDMA, and CDMA respectively). The current analog cellular system is AMPS (FDMA based). Personal Communications Services (PCS) is the name given to the newest generation of wireless services. Of the 2958 PCS licenses that were awarded in the USA in 1996, 51% were for IS-95 systems (CDMA based standard), 28% were for GSM systems(TDMA based standard), and 20% were for IS-136 systems(TDMA based standard)[1]. One can see that CDMA will play a major role in the increase of digital wireless services. Another attraction of CDMA is the fact that the FCC has allowed for unlicensed use of

the three Instrumentation, Scientific and Medical (ISM) bands with up to 1 Watt of output power for CDMA users. This is very attractive in a time where spectrum is auctioned for billions of dollars.

Diversity techniques can be employed to gain more efficient channel utilization. Diversity works by using two or more statistically independent copies of the same information. The use of these multiple copies of the information form a combined copy that is better than (or equal to) any of the original copies. Thus, use of diversity improves the reliability of the channel, requiring fewer retransmissions.

1.1 Significance of Research and Organization of Thesis

This dissertation examines the use of diversity techniques in improving the capacity and reliability of DS-CDMA wireless communications systems. It is separated into six chapters. In Chapter 2, some background material will be covered. This will assist the reader in understanding some of the concepts in the remaining chapters.

With wireless communications, we are faced with many different design restrictions. The wireless channel is plagued by many problems such as the reliability of the signal, capacity, privacy issues, and lack of spectrum. Diversity can improve the reliability and throughput of a wireless system without any increase in the bandwidth requirement. The cost one pays for these increases is in the complexity of the receiver. Thus, it is important to examine the trade offs between complexity and performance gain. In Chapter 3, these trade offs are examined for rake receiver structures in a DS-CDMA network. The results of the work in [2] are expanded to include generalized fading channels, using the Nakagami distribution. The performance of a finite branch

preselection maximal ratio combiner (MRC) receiver structure over Nakagami fading environments is investigated. In order to compare the performance versus complexity, a reduced tap MRC receiver, and the optimum linear diversity combiner are also investigated. The effects of different multipath intensity profiles (MIPs) is also explored for each of the receiver structures.

The properties of signal capture, multiple access, anti-multipath, and narrow-band interference rejection make DS-CDMA an excellent choice for use in packet data networks[3]. In Chapters 4 and 5 the performance of a DS-CDMA packet data networks is examined.

In Chapter 4, the performance of a DS-CDMA packet data network with Poisson generated traffic is analyzed. The throughput of a system using diversity is compared against a similar system with no diversity. The network uses a slotted ALOHA protocol with random back-off. Slotted ALOHA is chosen because of its ease of implementation. The simplicity of slotted ALOHA gives rise to the problems of low maximum throughput and unstability under high load. Slotted ALOHA discards packets in error and waits for a correct transmission of the desired packet. The packets in error can be used to increase the reliability of the subsequent transmitted packet. This is accomplished by combining the packets in error to produce a new packet, which is more reliable than any of the individual packets. The use of diversity packet combining can help improve the throughput and stability of the system.

The performance of a packet data network with diversity using self-similar traffic generation is investigated in Chapter 5. Several studies have found that Poisson modeling fails to accurately reflect the traffic patterns of some forms of traffic [4, 5, 6, 7].

They concluded that self-similar traffic more accurately reflects these traffic patterns. Chapter 5 compares the performance of a system with self-similar traffic with that of a system modeled with Poisson generated traffic. The effect of various MIPs and the effect of using a reduced complexity receiver is also examined. Chapter 6 contains conclusions and recommendations for future work.

Chapter 2 Background

Some background material that is common for all of the following chapters is discussed in this chapter. This information is useful for understanding some of the concepts in subsequent chapters.

2.1 Multipath Fading

Multipath fading, sometimes called short-term fading, is caused by the reflections of a transmitted radio signal. These reflections are caused by surrounding objects such as buildings, cars, trees, etc.. They can add up constructively or destructively. When the signals add destructively, the signal is attenuated. The resulting signal fluctuations caused by the addition of these reflections is called fading. The characteristics of the fades can be statistically modeled using random probability distributions. Different distributions are used depending on the environmental situation that one wishes to model. If a line of sight path is available between the transmitter and the receiver, that fading situation can be effectively modeled using the Rice probability density function (pdf) [8]. If no direct line of sight is available, the fading is usually modeled using Rayleigh pdf.

$$p(r) = \frac{2r}{\Omega} e^{-r^2/\Omega} \tag{2-1}$$

describes the Rayleigh pdf. This is a commonly used model for an outdoor channel.

The Nakagami *m*-distribution is another common channel model. It is described by [9],

$$p(r) = \frac{2}{\Gamma(m)}\left(\frac{m}{\Omega}\right)^{m} r^{2m-1} e^{-mr^2/\Omega}, \tag{2-2}$$

where m is the fading figure and Ω is the mean square value of the random variable. By varying the m parameter, it can be used to model a wide variety of channels. When m=1, the equation reduces to the Rayleigh pdf. By decreasing the value of m, the modeled channel will be more faded than that of Rayleigh modeled channel. By increasing *m,* the modeled channel becomes less faded than a Rayleigh modeled channel. As m approaches infinity, the modeled channel experiences no fading. If one is able to resolve different multipath signals, the collected group of signals is called a multipath intensity profile (MIP).

2.2 MIP

When receiving multipath signals, the signal strength of each of the resolvable multipaths is different. Furthermore, as subsequent multipath signals arrive, they are of less power than the previous signals. This is intuitively satisfying as the longer time the signal takes to arrive at the receiver, the more reflections it has undergone, and the longer the distance the signal has traveled. The multipath intensity profile (MIP) describes the collection of multipath signals. A common way of modeling MIP is through assuming an exponentially decaying MIP as follows:

$$\gamma_k = \gamma_1 e^{-(k-1)\delta}, \tag{2-3}$$

where δ in (2-3) is a positive constant that dictates the steepness of the multipath decay and γ_k is the SNR of the kth resolvable multipath.

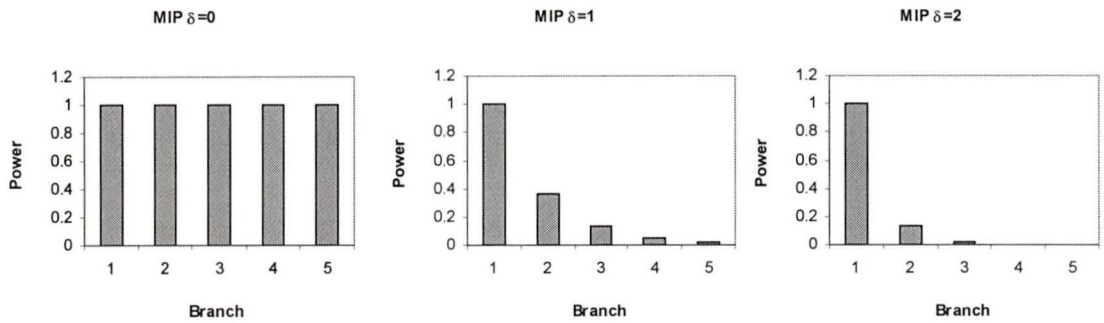

Figure 2-1. MIP for $\delta = 0$, 1, and 2.

From Figure 2-1, one can see that the amount of power available for capture with different MIPs is quite different.

2.3 Diversity

Diversity takes advantage of the statistically random nature of fading. Diversity schemes use two or more uncorrelated signals. The combination of these signals will always provide a better signal than that of a single signal. Therefore, the probability that the combined signal is incorrectly detected will be less than that of a single signal. Take for example the system of L switches controlling a single light, where the probability of a single switch failing is p. Each switch is capable of turning the light on or off. The probability that the light will be uncontrollable (all L switches failing) is p^L.

There are several diversity schemes that are used in wireless systems. These include space, frequency, polarization, angle, and time diversity. In this dissertation, only time and frequency diversity are considered.

2.3.1 Time Diversity

Time diversity works by sending L copies of the same signal, with more than the coherence time, Δt_c, in between each transmission. The coherence time is the minimum time interval between the transmission of two signals that will be independently faded. The coherence time is calculated by:

$$\Delta t_c = 1/\text{Doppler spread}. \tag{2-4}$$

Doppler spread is equal to the amount of frequency by which the signal bandwidth is spread as it passes through the channel.

In a packet data network, time diversity can work through the retransmission of failed packets. The time between transmissions will be much greater then the coherence time. Therefore, each retransmission of the packet will be independently faded.

2.3.2 Frequency Diversity

Another diversity method is frequency diversity. In this method, the same signal is transmitted on L different frequencies, where the separation between carriers is equal to or greater than the coherence bandwidth, Δf_c. Δf_c is the minimum frequency separation for statistically-independent fading. From [10] the coherence bandwidth is calculated by:

$$\Delta f_c = 1/(2 \pi \tau_d), \tag{2-5}$$

where τ_d is the time delay spread. For different man-made environments, approximate time delay spreads have been calculated.

Environment	Time Delay Spread, τ_d (μs)
urban areas	3
suburban areas	0.5
open areas	0.2

Table 2-1 Time delay spread for different environments.

After all of the diversity branches are collected, the signals must go through some form of combining before detection. There are four major types of combining. These are: switched, selective, equal gain, and maximal ratio. In switched combining, only two input diversity signals are used. The first signal is used until it falls below some threshold level. At that time the second signal is used. When the second signal falls below the threshold the first signal is used again. This continues until the transmission is completed. With selective combining the receiver chooses the strongest of the input signals to pass to the detection stage. When equal gain combining is used, all of the diversity branches are co-phased and then summed together. Maximal ratio combining is the optimum combining technique. Each of the input diversity branches are co-phased, weighed in proportion to their SNR, and then summed.

2.4 Rake Receiver

A rake receiver uses frequency diversity and maximal ratio combining. The frequency diversity comes from the transmission of a wide band signal in a frequency selective channel. In such a situation we can use the tapped delay line model for the channel. This is illustrated in Figure 2-2, where W is the bandwidth of the signal ($W>>\Delta f_c$), $\alpha_i(t)$ are complex valued with Rayleigh distributed magnitudes and uniformly

distributed phases, and n(t) is additive white Gaussian noise. (The value of $\alpha_i(t)$ can also follow the other distributions mentioned in section 2.1.) The rake receiver is able to extract a finite number of the resolvable multipaths, and pass them on to the MRC. The error probability when using a rake receiver is

$$P = \frac{1}{2}\sum_{k=1}^{L}\pi_k\left[1-\sqrt{\frac{\bar{\gamma}_k(1-\rho_r)}{2+\bar{\gamma}_k(1-\rho_r)}}\right] \tag{2-6}$$

where

$$\pi_k = \prod_{\substack{i=1 \\ i\neq k}}^{L}\frac{\bar{\gamma}_k}{\bar{\gamma}_k-\bar{\gamma}_i},$$

$\bar{\gamma}_k$ = average SNR for the kth branch, and ρ_r = -1 for BPSK signals. Recall that from section 2.2, each successive branch follows the MIP. A rake receiver is depicted in Figure 3-3. Rake receivers are commonly used in Spread Spectrum systems.

2.5 Spread Spectrum

Spread Spectrum (SS) techniques use a transmission bandwidth many times greater than the minimum bandwidth required to transmit the information. SS signals are multiplied by a pseudo-random signal unique for each user. The receiver despreads the signal by correlating the received SS signal with its unique pseudo-random sequence. Some of the benefits of SS systems are signal capture, anti-multipath, privacy, soft handoff, interference suppression, energy density reduction, and multiple access capability. These reasons are why SS has been a popular choice in military and commercial wireless systems.

There are four aspects of SS that can be exploited for packet data networks [3]. These include signal capture, multiple access, anti-multipath, and narrow-band interference rejection. The capture effect is the ability to demodulate a single signal from a group of overlapping signals. Good capture ability can greatly improve delay and throughput performance of the packet network [11]. Multiple-access refers to the ability of the receiver to receive packets addressed to it in the presence of interference created by other packets being sent by other users at the same time. The use of a unique pseudo-random sequence for each of the users allows them to decode the messages transmitted for an individual user. Anti-multipath refers to the ability to combat multipath interference. Narrow-band interference rejection is the ability to successfully receive a packet in the presence of narrow-band jamming or other types of radio transmissions.

2.6 ATM

Asynchronous Transfer Mode (ATM) is a cell based technology designed to operate a general purpose, connection-oriented network. ATM was designed to handle a wide variety of traffic types, including audio, data, and video. There has been a push to develop wireless ATM to interface to its wire line version[12]. ATM can handle connectionless traffic through its adaptation layers. ATM has five ATM Adaptation Layers (AALs) to handle the four classes of service. These are described in Table 2-2 and Table 2-1.

AAL1	AAL that is used to provide class A service.
AAL2	AAL that is used to provide class B service.
AAL3/4	AAL that is used to provide class C and D service.
AAL5	AAL that is used to provide class C and D service, but is more streamlined than AAL 3/4.

Table 2-2. AAL descriptions

Class A	Connection oriented constant bit rate (CBR) service. (eg. Voice, fixed rate video)
Class B	Connection oriented variable bit rate (VBR) service. Bounded delay. (eg. Compressed video)
Class C	Connection oriented available bit rate (ABR) service. Unbounded delay. (eg file transfer)
Class D	Connectionless ABR service. (eg datagrams)

Table 2-3. ATM Class descriptions.

For each class of traffic, a different method of modeling the traffic must be used.

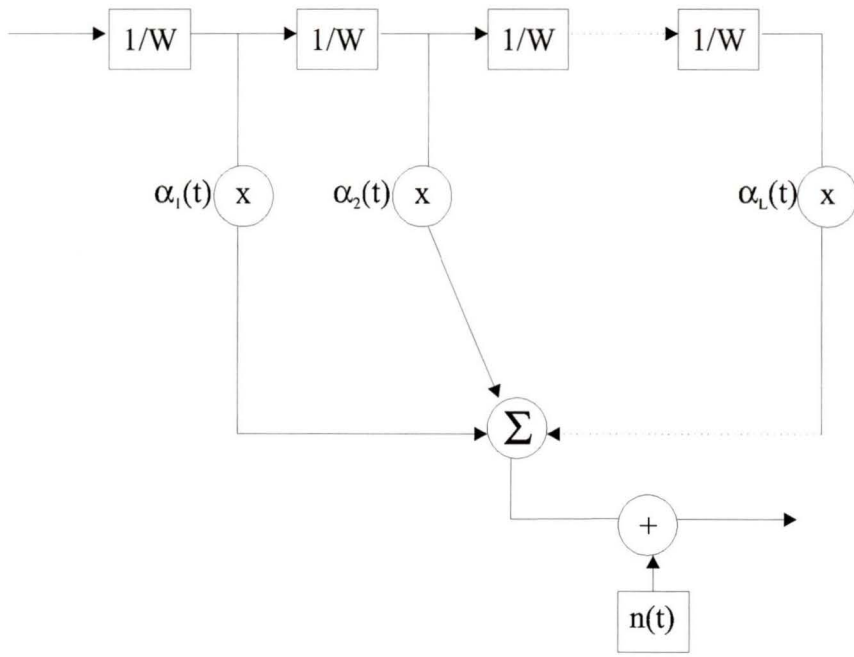

Figure 2-2. Tapped delay line model for frequency selective channel.

Chapter 3 Rake Receiver Structures

3.1 INTRODUCTION

Rake reception is an excellent strategy to exploit the autocorrelation properties of the PN spreading signature waveforms, by resolving and combining the multipath components to obtain multipath diversity [13]. Various diversity combining techniques may be employed to achieve a good compromise between performance and implementation complexity. While multipath allows us to gain diversity advantage, it also has the undesirable effect of accentuating the interference from multiple-access. In light of these considerations, several methods of diversity combining are evaluated and compared for a coherent DS/CDMA system.

In this chapter, the analysis presented in [2] is extended by studying the performance of an M-SCMRC receiver structure over Nakagami fading environments. Additionally, the performance of a reduced-complexity rake receiver with finite taps (fingers), and the optimum linear diversity combiner are investigated for comparison.

3.2 SYSTEM DESCRIPTION

Our interest in the signal begins at the receiver, so the analysis of the system starts with the signal at the receiver. The received faded signal can be written as:

$$r(t) = \mathrm{Re}\left\{R(t)e^{j\omega_c t}\right\} \tag{3-1}$$

where,

$$R(t) = \sum_{i=1}^{L} \alpha_i e^{j\theta_i} S_i(t) + N(t) \tag{3-2}$$

and where $\{\alpha_i\}$ are Nakagami-distributed, and $\{\theta_i\}$ are the uniformly distributed phases.

The transmitted DS/CDMA signal is degraded by self-interference, channel attenuation due to multipath fading, multi-user interference, and additive white Gaussian noise. In order to capture the signal from user *i*, the received composite signal is assumed to go through a rake receiver with M taps (fingers), where $M \leq L$, and L corresponds to the maximum number of resolvable multipaths. First, the received signal is despread independently for each multipath component, by multiplying the signal by the spreading signature code for the *i*th user, delayed by an amount equal to the estimated multipath delay. The modulated signal is then down-converted to a baseband signal and passed through a bank of correlators prior to diversity combining. In the maximal-ratio combiner, the voltage signals from each of the M path diversity branches are first co-phased, and then weighted in proportion to their signal level before summing. The sampled decision statistic at the output of the rake demodulator is then passed through a threshold detector where a hard decision for the bit is made.

There are three different rake demodulators under investigation. These are shown in Figure 3-1, Figure 3-2, and Figure 3-3. Figure 3-3 shows the optimum rake demodulator (L-MRC). At the intermediate or baseband frequency, all of the resolvable multipaths, L, are correlated with the delayed signature waveforms and passed on to a maximal ratio combiner, with the number of input taps equal to the total number of resolvable multipaths of the original signal. Figure 3-1 shows a rake demodulator with finite tap decisions (M-MRC). Instead of all resolvable multipaths being passed on to a

maximal ratio combiner, only a finite number is passed on. This is a more practical situation, as the receiver structure is fixed and the number of resolvable multipaths in a real channel is time varying. Figure 3-2 shows a pre-selection maximal ratio combining rake demodulator (M-SCMRC). This receiver enhances the performance of the M-MRC receiver. This is done by selecting the best M signals out of all of the resolvable multipaths and passing them onto a maximal ratio combiner.

3.3 ANALYSIS

The bit error rate performance depends on the type of diversity combining being used, and the channel conditions. In practice, the number of tap decisions used in a rake receiver, M, can be less than the channel length, L, with some sacrifice of performance. Notice that L corresponds to the number of taps in the discrete-time channel model (see Figure 1). With the assumption of an exponentially decaying multipath delay profile, the mean received signal-to-noise ratio for the kth path is,

$$\bar{\gamma}_k = \frac{1-e^{-\delta}}{e^{-\delta(k-1)}\left(1-e^{-\delta L}\right)}\bar{\gamma}_b \tag{3-3}$$

where δ denotes the decay rate, and $\bar{\gamma}_b = \sum_{l=1}^{L}\bar{\gamma}_l$ corresponds to the average total received signal-to-noise ratio (usually referred to as SNR per bit).

3.3.1 Optimum Linear Diversity Combiner (L-MRC)

Maximal-ratio combining is known to be optimum in the sense that it yields the best statistical reduction of fading in any linear diversity combiner. In this technique, all of the L time-diversity branches are first co-phased and then weighted in proportion to

their signal level before summing. Using the usual approach of computing the characteristic function of γ_{mrc} as the product of the statistically independent random variables, and then followed by an inverse Fourier transformation to obtain the p.d.f., we obtain the average probability of bit error in the form [14],

$$P_b = \sum_{k=1}^{L}\sum_{q=1}^{m} A_{kq}\left[\frac{1-\mu_k}{2}\right]^q \sum_{i=0}^{q-1}\binom{q-1+i}{i}\left[\frac{1+\mu_k}{2}\right]^i \tag{3-4}$$

where , $\mu_k = \sqrt{\dfrac{\bar{\gamma}_k}{m+\bar{\gamma}_k}}$, m denotes the fading figure [8], and A_{kq} is defined as

$$A_{kq} = \frac{1}{(m-q)!\left(\dfrac{\bar{\gamma}_k}{m}\right)^{m-q}} \frac{d^{m-q}}{ds^{m-q}} \left\{ \prod_{\substack{i=1 \\ i\neq k}}^{L} \left[1 - \frac{s\bar{\gamma}_i}{m}\right]^{-m} \right\}\Bigg|_{s=\frac{m}{\bar{\gamma}_k}} \tag{3-5}$$

For a uniform multipath intensity profile, (3-4) can be re-stated as [14],

$$P_b = \left[\frac{1-\mu}{2}\right]^{mL} \sum_{k=0}^{mL-1}\binom{mL-1+k}{k}\left[\frac{1+\mu}{2}\right]^k \tag{3-6}$$

Notice that when m=1, the bit error rate formulas described by (3-4) and (3-6) for the L-diversity maximal-ratio combiner in Rayleigh fading are equivalent to the expressions given in [8, 14-5-28] and [8, 14-4-15], respectively. Moreover, when m=1 and L=1, (3-6) reduces to the familiar expression for P_b in Rayleigh fading channel with no diversity. A more detailed treatment of the calculation of (3-4) can be found in Appendix A.

3.3.2 Maximal-Ratio Combiner with Finite-Tap Decisions (M-MRC)

An M-MRC receiver structure (refer to Figure 3-1) differs from the optimum linear diversity combiner because only the first M tap-decisions ($M<L$) are captured to form the overall decision statistics. Hence, the bit error rate performance of this inferior receiver configuration is given by (3-4) and (3-6), substituting L with M. By choosing different values of M, the trade off between performance and receiver complexity can be investigated. For instance, the performance of a single correlator receiver in different fading environments can be readily evaluated by setting M=1. On the other hand, by selecting M=L, performance of the optimum coherent receiver is realized.

3.3.3 Pre-Selection Maximal-Ratio Combiner (M-SCMRC)

In an M-SCMRC system, a rake receiver utilizes multiple correlators to detect separately the M strongest multipath components. The bit decisions are then based on the weighted output of these M strongest signals. Intuitively, the performance of this receiver configuration will be superior than that of an M-MRC system because we attempt to enhance the reliability of the decision statistics by combining the strongest M multipath signals, instead of just capturing the first M multipath signal arrivals. However, it should be noted that this improvement is achieved at the expense of increased processing complexity. The average probability of bit error of an M-SCMRC rake receiver is,

$$P_b = \int_0^{\infty}\int_{y_2}^{\infty}\cdots\int_{y_M}^{\infty} \frac{1}{2} erfc\left(\sqrt{y_1 + y_2 \ldots + y_M}\right) f_{\gamma_1,\gamma_2,\ldots,\gamma_M} dy_1 dy_2 \ldots dy_M \tag{3-7}$$

where the joint probability density function is given by,

$$f_{\gamma_1,\gamma_2,..,\gamma_M}(y_1,y_2,...,y_M)=\sum_{i=1}^{L} f_{\gamma_i}(y_1)\sum_{\substack{j=1\\ j\neq i}}^{L} f_{\gamma_j}(y_2)...\sum_{\substack{z=1\\ z\neq i,j,...}}^{L} f_{\gamma_z}(y_M)\prod_{\substack{a=1\\ a\neq i,j,...,z}}^{L} F_{\gamma_a}(y_M) \tag{3-8}$$

with $f_{\gamma_j}(y)$ and $F_{\gamma_j}(x)$ defined as,

$$f_{\gamma_j}(y)=\frac{m^m}{\Gamma(m)\bar{\gamma}_j{}^m}y^{m-1}\exp\left(\frac{-my}{\bar{\gamma}_j}\right) \tag{3-9}$$

$$F_{\gamma_j}=\frac{m^m}{\bar{\gamma}_j{}^m\Gamma(m)}\int_0^x y^{m-1}exp\left(\frac{-my}{\bar{\gamma}_j{}^m}\right)dy$$

$$=1-exp\left(\frac{-mx}{\bar{\gamma}_j{}^m}\right)\sum_{k=0}^{m-1}\frac{1}{k!}\left(\frac{mx}{\bar{\gamma}_j{}^m}\right)^k, m\in\{integer\} \tag{3-10}$$

A closed-form expression for this combining scheme on a Rayleigh-faded channel is derived in [2].

3.4 COMPUTATIONAL RESULTS AND REMARKS

In the following graphs, the channel length, L, is assumed to be 5. Three variations of a rake receiver are evaluated on a Nakagami-faded environment based on the bit-error rate expressions presented in the preceding section. It is worth noting that the approximate bit error rate expression found in [15] is only exact when δ=0, and its accuracy deviates from the actual error performance as δ increases. However, the formula described by (3-4) is exact even when the mean signal strengths of the multipath signals have a large variance, i.e., an exponential multipath intensity profile (MIP) with a large decay rate factor. An alternative probability density function for γ_{mrc} is outlined in [16], but the result is in the form of an integral; therefore, a numerical integration method has to be employed to approximate the final result.

Figure 3-4 and Figure 3-5 depict the bit error performance of the three receiver configurations (illustrated in Figure 3-1, Figure 3-2, and Figure 3-3) for different multipath intensity decaying rates and varying channel conditions. From Figure 3-4, it appears that in a Rayleigh-faded environment, the performance of a 3-SCMRC system is much closer to the optimal coherent receiver than the 3-MRC scheme. This is attributed to the improved statistics of the combined signal by selecting the best three multipath signals, instead of simply capturing the first three arrivals. Similar trends were observed in [2]. However, the difference between the M-SCMRC and L-MRC becomes more appreciable as the channel condition improves (with moderate or small δ). A comparison between Figure 3-4 and Figure 3-5 reveals that the discrepancy between the three combination methods diminishes as the channel becomes less dispersive (i.e., as δ increases). This is intuitively satisfying because only a small amount of multipath diversity can be attained from a frequency nonselective channel. The observation is also valid in the presence of a strong direct-path component.

Figure 3-6 exhibits the gain that can be realized by combining additional multipath signals as a function of the power distribution profile and the fading figure. While the probability of deep fades decreases as the number of independent diversity receptions increases, the marginal value of higher order diversities diminishes. For the same reason, diversity improvement diminishes as the channel condition improves (higher m). The improvement exhibited in a uniform multipath intensity profile (corresponding to δ=0) scenario owes to the following two factors: (i) the total power captured by combining additional multipaths, and (ii) diversity gain by having more statistically independent diversity branches. In contrast, the improvement noticed in a

heavily decayed multipath intensity profile situation is mainly contributed by the diversity gain alone, since most of the power has been captured in the leading path. In particular, the trend in Figure 3-6(b) clearly illustrates the contribution of these two factors in different fading environments. It is evident that the power capture has a stronger influence in less severely faded environments with uniform MIP, while diversity gain is a more predominant factor as δ gets larger, with poorer channel conditions.

In practice, the diversity improvement attained by combining many demodulator fingers actually declines beyond some optimal value, as each demodulator finger already has improved statistics, and because of the surmounting combination losses of many fingers. Therefore, M-MRC and M-SCMRC are viable candidates for the realization of a low-complexity rake receiver. Additionally, it is shown that the optimum number of combined branches is dictated by the acceptable receiver complexity and the multipath intensity profile.

In Table 3-1 the amount of power capture and the diversity gains over no combining are shown. The percentage of power captured by additional diversity branches and the performance over no combining are for an uncoded bit error probability of 10^{-2}. The no combining performance is obtained from a single multipath containing the same power as the total of the five resolvable multipaths. From Table 3-1, one can see that there is more gain over no diversity for poorer channel conditions. Also, the performance gain versus no combining of flatter MIPs is better than that of more steeply decaying MIPs. The flatter the MIP, the more one gains from additional diversity branch because of the increased reliability of the subsequent independently faded branches.

3.5 Conclusions

In this chapter the efficacy of M-SCMRC, M-MRC, and L-MRC rake receivers is compared in different fading environments. The results reveal that M-SCMRC outperforms M-MRC and performs closely to L-MRC in most situations. When the channel becomes less dispersive (larger δ), the differences in the three methods becomes less apparent. This can be attributed to the fact that most of the power comes from the first resolvable multipath, additional branches have only a minor effect on performance. The gain of diversity was found to diminish as the channel conditions improve. It was also found that as the decay factor, δ, increases, the gain of adding additional diversity branches diminishes.

δ	Branches	Power Captured	Diversity Gain Over no combining [m=1] (dB)	Diversity Gain Over no combining [m=2] (dB)
0.0	1	20.00%	4.27	-1.07
	2	40.00%	6.47	1.31
	3	60.00%	7.43	2.46
	5	100.00%	8.07	3.43
0.5	1	42.87%	4.03	-0.72
	2	68.86%	6.12	1.46
	3	84.63%	6.99	2.41
	5	100.00%	7.55	3.13
1.0	1	63.64%	3.63	-0.28
	2	87.05%	5.50	1.60
	3	95.67%	6.16	2.24
	5	100.00%	6.51	2.55
2.0	1	86.47%	2.54	-0.14
	2	98.17%	4.04	1.24
	3	99.76%	4.35	1.43
	5	100.00%	4.43	1.47

Table 3-1. Power Capture and gain over no combining versus number of branches combined and MIP decay rate.

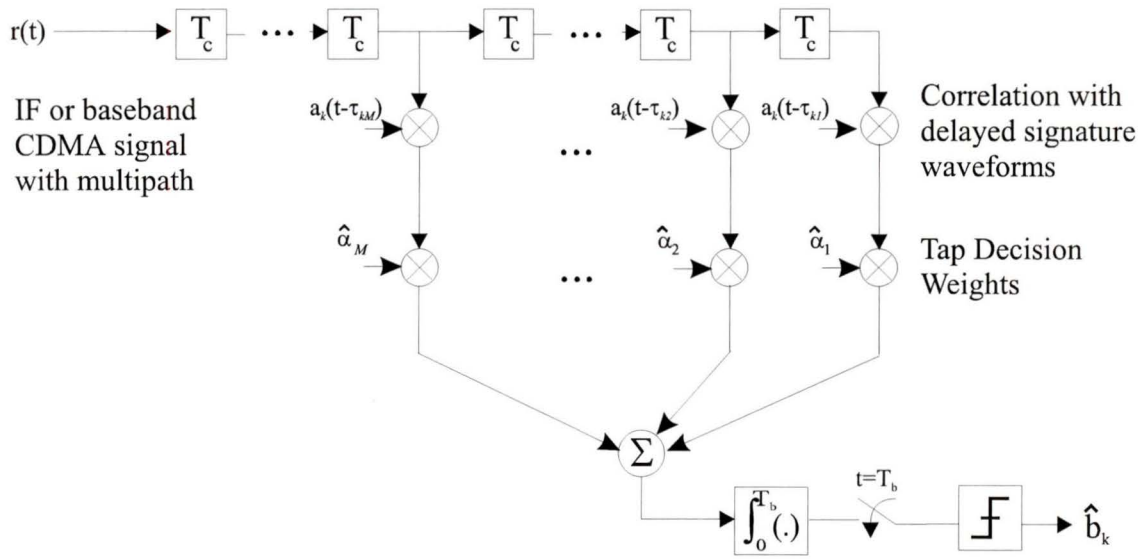

Figure 3-1 Rake Demodulator with Finite-Tap Decisions (M-MRC)

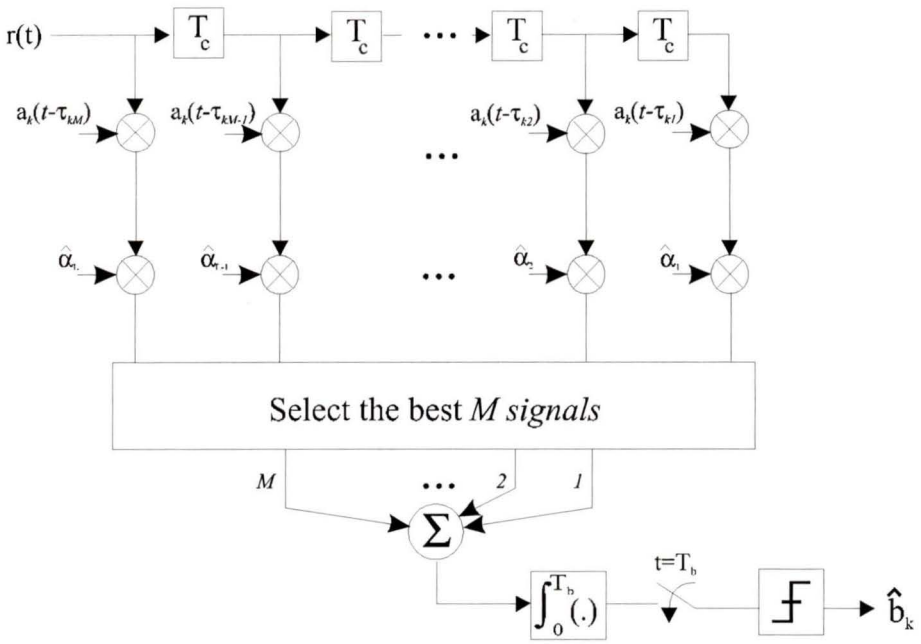

Figure 3-2. Pre-selection Maximal-Ratio Combining Rake Demodulator (M-SCMRC)

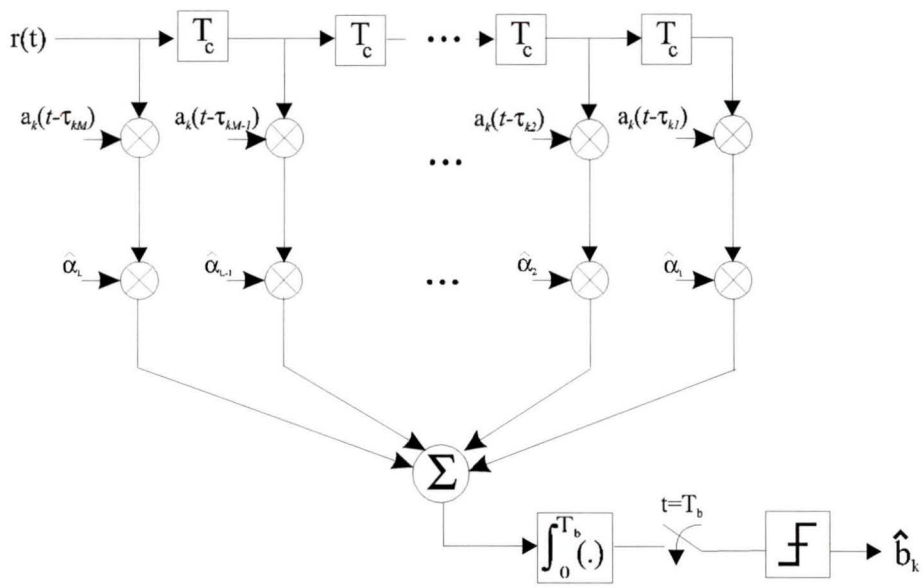

Figure 3-3. Optimum Rake Demodulator for Coherent DS/BPSK signals (L-MRC)

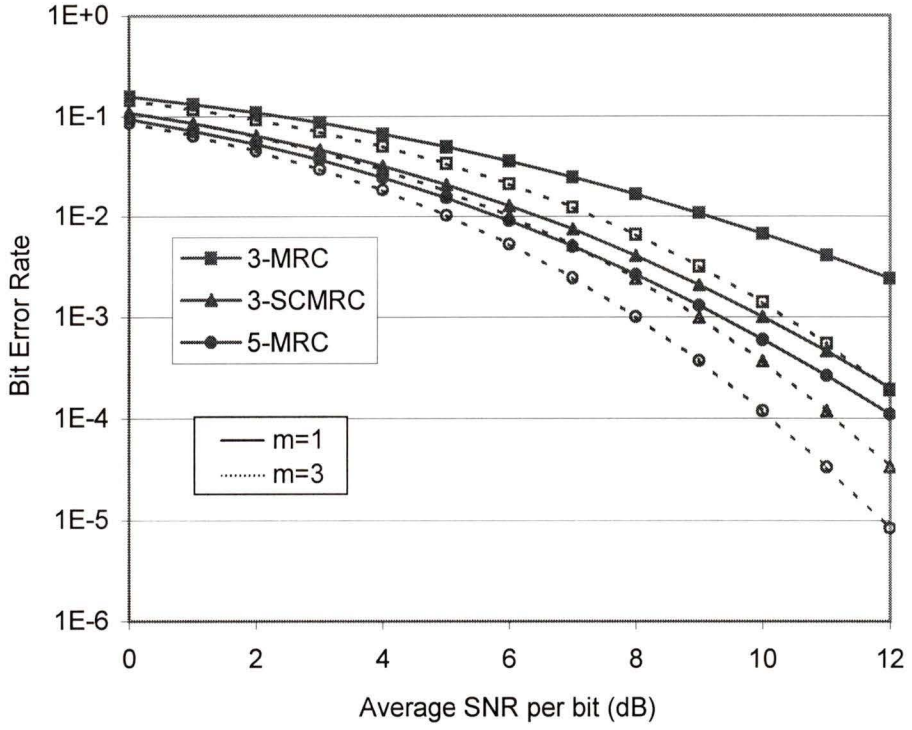

Figure 3-4 Comparison of different rake receiver structures for coherently detected DS/BPSK systems with δ=0 (uniform MIP) over two fading environments.

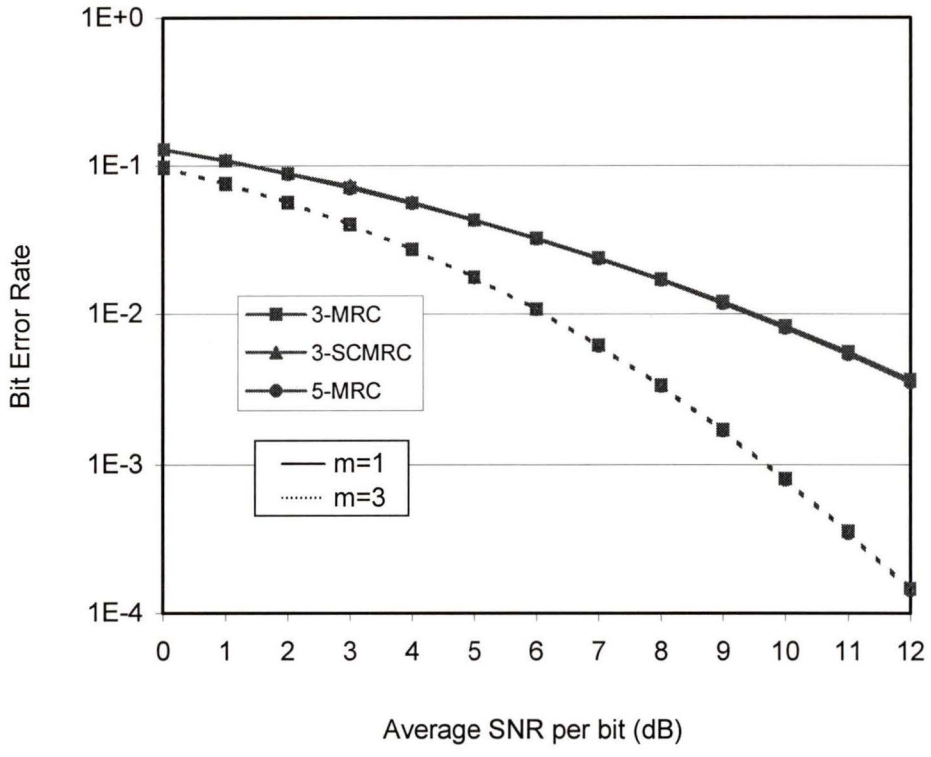

Figure 3-5. Comparison of different rake receiver structures for coherently detected DS/BPSK systems with δ=2 (exponential MIP) over two fading environments.

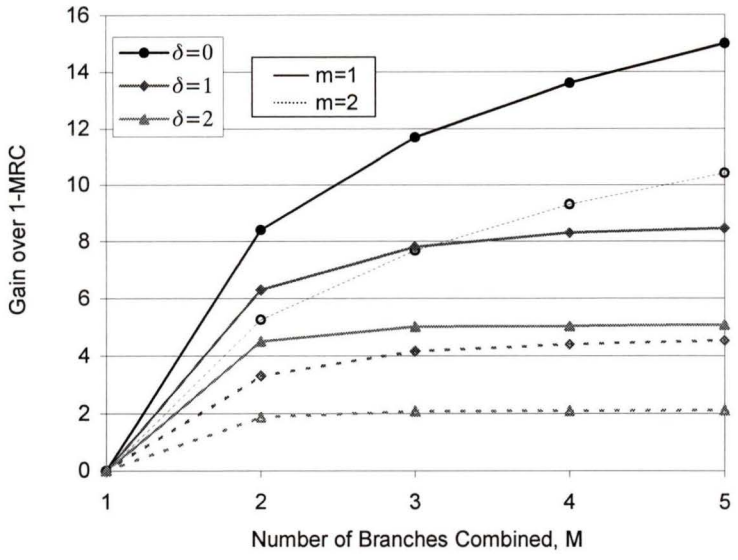

(a) M-MRC

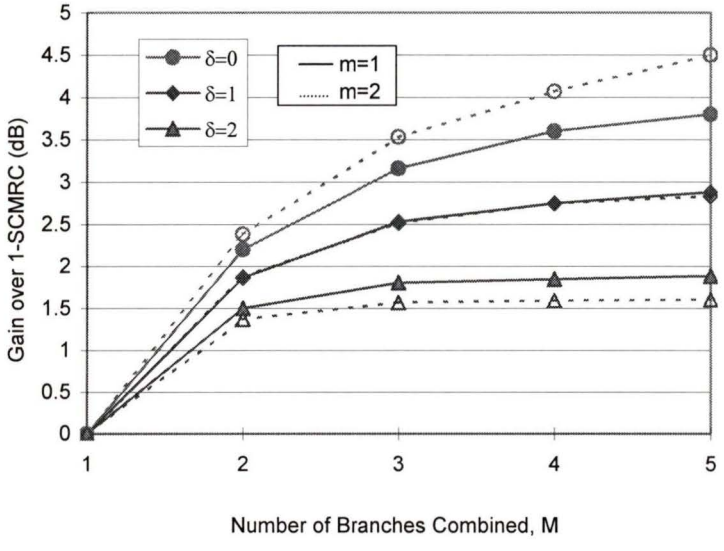

(b) M-SCMRC

Figure 3-6. The gain of combining additional time diversity branches over a single multipath signal at BER= 10^{-2}

Chapter 4 Poisson Modeled Packet Data with Packet Diversity

The goal of integrated networks is to provide a single transport for all types of traffic, be it voice, video, or data. Such a scheme would have the advantage of variable data rates and thus allow the user to use as much or as little bandwidth as their application required. Furthermore, since such a system is dynamic, future applications should be easy to integrate into the network. The challenge is to find the best wireless system to implement the network. One possible candidate is a simple random access protocol like ALOHA. Its major advantage is that it can be implemented with relativity little complexity. Unfortunately, pure ALOHA is plagued by low maximum throughput and unstability under high load. Diversity can help improve the throughput and stability of the system. This chapter investigates the performance of such a system.

4.1 System Description

4.1.1 Packet Data Generation

Slotted ALOHA is one of the simplest of all access schemes. The time at which users can transmit is broken up into time slots. A simplified example would be that if it took 1 second to transmit a packet, users could only transmit at the beginning of each second. Therefore, packet transmissions will either completely overlap each other (multiple users send at once) or not overlap all. Users can transmit packets in any time slot they wish. After a message has been transmitted, the user listens for an

acknowledgment (ACK) or a negative acknowledgment (NAK) from the receiver for the transmitted packet. An ACK tells the user that the packet was successfully received. When a NAK is received (or the absence of an ACK) by the user, the packet is assumed to have failed. The packet is then retransmitted. In a non-CDMA system, when two or more users send a packet in the same time slot, the packets collide and all of transmissions fail. In a CDMA system two or more users can send packets simultaneously without necessarily resulting in the failure of all of them. The packets in a CDMA system only experience an increase in the multiple access interference.

In this chapter, the traffic for the system is generated using a Poisson distribution. Processes that follow the Poisson model have an exponential inter-arrival time between each of the events. Retransmissions of packets have a random, exponentially distributed, inter-arrival time from the reception of the NAK. From [17] the composite packet arrival distribution $f_g(m)$ is given by,

$$f_g(m) = \frac{(\lambda T)^m}{m!} e^{-\lambda T}, \tag{4-1}$$

with λ, the composite arrival rate and T, the packet reception interval.

Forward error correction (FEC) is used in all of the systems investigated. The codes are 127 bit long BCH codes. The exact codes used are shown in Table 4-1, where n is equal to the total number of bits in the block code, k is the number of data bits, and t is the number of correctable bits [18].

n	k	t
127	127	0
127	113	2
127	106	3
127	99	4
127	92	5

Table 4-1. BCH Codes

4.1.2 Channel Model

Since we are only interested in the signal at the receiver, our analysis shall begin there. The received signal can be represented by

$$r(t) = \mathrm{Re}[R(t)e^{j\omega_c t}] \tag{4-2}$$

where,

$$R(t) = \sum_{i=1}^{L} \alpha_i e^{j\theta_i} S_i(t) + N(t) \tag{4-3}$$

and where $\{\alpha_i\}$ are Rayleigh-distributed signal amplitudes, and $\{\theta_i\}$ are the uniformly distributed phases. $S_i(t)$ represents the low-pass modulated signal from branch i, and $N(t)$ represents the complex valued AWGN, with a double-sided spectral density, η_o.

The transmitted DS-CDMA packet is degraded by self-interference, channel attenuation due to multipath fading, multi-user interference, and additive white Gaussian noise. In order to capture the signal from user i, the received composite signal is assumed to go through a rake receiver with M taps (fingers), where $M \leq L$, and L corresponds to the maximum number of resolvable multipaths. The sampled signals, at the output of the rake demodulator, but before the hard decision stage, for each of the received packets, is

stored in a register. The packet is held in the register until it is found to contain no errors or a correctable error pattern. If the packet is uncorrectable, a retransmission request is sent. The second copy of the packet is then subject to the same procedure. If it is found to be correct or correctable, the first copy is deleted from the register. If the second copy is found to be incorrect, it is bit by bit combined together with the previous transmission. This continues until the packet is successfully received or the maximum number of transmissions has been reached.

The instantaneous received signal to noise ratio (SNR) is defined as,

$$\gamma_b = \sum_{q=1}^{I} \sum_{k=1}^{M} \gamma_{qk} \tag{4-4}$$

where I is the number of transmissions of the same packet that have been received, and M is the number of fingers in the rake receiver. The value for $\bar{\gamma}_k$, the average SNR for path k is approximated by [19],

$$\bar{\gamma}_k \cong \frac{E[\beta_k^2]}{\frac{2}{3N}\sum_{\substack{j=1 \\ j\neq k}}^{L} E\left[\beta_j^2\right] + \frac{2K}{3N}\sum_{j=1}^{L} E\left[\beta_j^2\right] + \frac{N_o}{E_b}} \tag{4-5}$$

where N is the processing gain, K is the number of additional users, L is total number of resolvable multipaths, and β_j is equal to the channel gain of the jth path. Since,

$$E[\beta_j] = E[\beta_1] e^{-(j-1)\delta} \tag{4-6}$$

when exponentially decaying MIP is assumed, the average SNR for each path can be simplified to,

$$\bar{\gamma}_k = \left[\frac{2(K+1)}{3N} \sum_{\substack{j=1 \\ j \neq k}}^{L} e^{-(j-k)\delta} + \frac{2K}{3N} + \frac{N_o}{E_b E[\beta_k^2]} e^{-(k-1)\delta} \right]^{-1}. \tag{4-7}$$

The variable δ represents the decay rate of the MIP.

4.2 Results

The probability of bit error with *m* packets being sent at that time and *I*th order diversity is,

$$P_i(m) = \sum_{k=1}^{M} \sum_{q=1}^{I} A_{kq} \int_0^{\infty} \frac{1}{2} erfc\left(\sqrt{x}\right) \frac{x^{q-1}}{(q-1)!\bar{\gamma}_k{}^q} e^{-x/\bar{\gamma}_k} dx \tag{4-8}$$

where

$$\int_0^{\infty} \frac{1}{2} erfc\left(\sqrt{x}\right) \frac{x^{q-1}}{(q-1)!\bar{\gamma}_k{}^q} e^{-x/\bar{\gamma}_k} dx = \left[\frac{1-\mu_k}{2}\right]^q \sum_{i=0}^{q-1} \binom{q-1+i}{i} \left[\frac{1+\mu_k}{2}\right]^i, \tag{4-9}$$

$$A_{kq} = \frac{1}{(I-q)!(-\bar{\gamma}_k)^{I-q}} \frac{d^{I-q}}{ds^{I-q}} \left\{ \prod_{\substack{i=1 \\ i \neq k}}^{M} [1 - s\bar{\gamma}_i]^{-I} \right\} \Bigg|_{s=\frac{1}{\bar{\gamma}_k}}, \tag{4-10}$$

and

$$\mu_k = \sqrt{\frac{\bar{\gamma}_k}{m+\bar{\gamma}_k}}. \tag{4-11}$$

The value for $\bar{\gamma}_k$ is given in (4-7). The probability of block error is given by,

$$Pb_i(m) = 1 - \sum_{x=0}^{t} \binom{N_p}{x} P_i(m+1)^x \left[1 - P_i(m+1)\right]^{N_p - x} \tag{4-12}$$

where t is the error correction capability and N_p is the number of bits per packet.

In order for us to compare with other packet data systems, the results must be normalized to the channel utilization efficiency. The throughput results presented in this chapter are shown for normalized throughput η:

$$\eta = \frac{\chi k}{R_{av} N n}, \tag{4-13}$$

where R_{av} is the average number of transmissions for a packet, k/n is the coding rate, N is the processing gain, and χ is the average number of packets generated during the time slot. The absolute upper and lower bounds on normalized throughput can be calculated by using the absolute lower (4-15) and upper bounds (4-14) on the average number of transmissions respectively in (4-13).

$$R_{av-AU} = 1 + \sum_{i=1}^{\infty} \sum_{m=0}^{\infty} \left\{ \left[\sum_{s=0}^{m} f_g(s) \right]^i - \left[\sum_{s=0}^{m-1} f_g(s) \right]^i \right\} Pb_i \tag{4-14}$$

and

$$R_{av-AL} = 1 + \sum_{i=1}^{\infty} \sum_{m=0}^{\infty} \left\{ \left[1 - \sum_{s=0}^{m-1} f_g(s) \right]^i - \left[1 - \sum_{s=0}^{m} f_g(s) \right]^i \right\} Pb_1^{\,i-1} \prod_{j=1}^{i} Pb_j \tag{4-15}$$

respectively.

The absolute lower bound of normalized throughput for five different coding rates can be seen in Figure 4-1(a) and the absolute upper bound on the average number of transmissions is shown in Figure 4-1(b). A closer examination of Figure 4-1(a) shows that the normalized throughput for the different FEC codes cross over each other. The cross over point corresponds very well with the effects of combining. If we take the example of the lines that represent t=3 and t=4, we see that they cross each other at an offered traffic of approximately 55 and 65. These values correspond well with the points

at which the lines that represent t=3 and t=4 cross 2 average transmissions in Figure 4-1(b). This can be explained by the fact that when the average number of transmissions crosses 2, the 2 corrupted packets can be combined to produce a correctable packet. This improves the normalized throughput and thus results in a cross-over. When the t=3 series crosses the t=4 series at an offered traffic of approximately 55, the average number of transmissions for t=3 crosses 2. This means that the performance of a 3 error correcting code with packet combining has a higher normalized throughput than a 4 error correcting code with no packet combining. Recall that packet combining requires 2 or more corrupted packets (i.e. an average of 2 or more transmissions). The two lines cross again at about an offered traffic of 65, the point at which the average number of transmissions for t=4 crosses 2. The plots for the absolute upper bound on normalized throughput and the absolute lower bound on average number of transmissions can be seen in Figure 4-2(a) and Figure 4-2(b) respectively.

In Figure 4-3 the delay-throughput analysis for different FEC code rates is investigated. For the non-combining cases, we see the expected curve for ALOHA systems. The normalized throughput increases sharply with the small corresponding increase in the average number of transmissions. This occurs until the channel is saturated and throughput begins to decline. For the combining cases, the saturation point is much higher. It is also important to note the "bends" in the curves as they cross an average number of transmissions of 2. This increase in performance can be attributed to the fact that as the curves cross 2, the average transmission performs combining. This is the same observation was made from Figure 4-1 and Figure 4-2, when the curves crossed over.

From Figure 4-4, the effect of different MIP is investigated. The highest normalized throughput can be achieved with δ=0 (all the received multipaths have the same average signal strength). The improvement can be attributed to the amount of power captured and the fact that that power is spread over all of the branches. The amount of improvement from diversity is higher because of the higher reliability of each of the additional branches. The improvement from diversity is maximized when the statistically independent branches have the same average signal strength. The reduction in throughput from δ=1 and δ=2 can be attributed to the same reasons. As the MIP decay rate increases, the channel becomes less dispersive, and the diversity gains are reduced.

The results displayed in Figure 4-5 would seem to contradict the results from Figure 4-4. The important difference to remember is that in Figure 4-5 there are only three of the five multipaths being passed to the MRC. This is a significant drop in power captured for the δ=0 case. For the more heavily decayed MIP situations, the effect of selecting only the first three of the multipaths is minimal. When one compares the performance of the δ=2 case in Figure 4-4 and Figure 4-5, they are almost identical.

4.3 Conclusions

The performance of a wireless packet data system with Poisson modeled traffic with and without packet combining was investigated. The combining is performed at the bit level using an MRC. Analytical expressions for calculating the average number of transmissions and the normalized throughput were presented. The numerical results show that the packet data system has significantly higher normalized throughput with the use of packet combining than without combining. The use of FEC can further enhance

the normalized throughput performance by reducing the average number of transmissions. The effects of different channel multipath profiles showed that the normalized throughput was higher for smaller δ (flatter multipath profiles). Simplifying the rake receiver by reducing the number of fingers showed that with the reduced number of paths captured, the flatter multipath profiles suffered from the reduction in power captured. The effects of reducing the number of fingers with larger δ (more steeply decaying MIP) is minimal. This means that for a channel with a large MIP decay rate, the advantage of having many fingers on the rake receiver is heavily reduced.

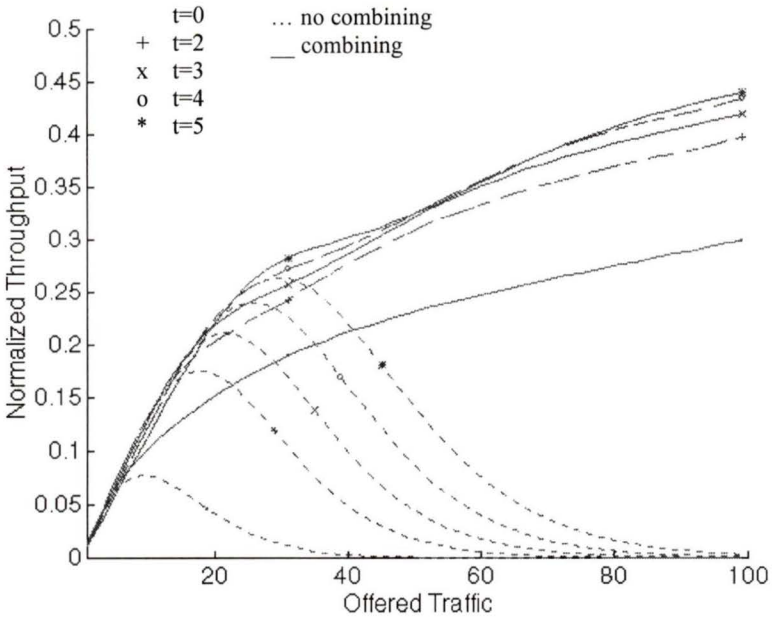

(a)

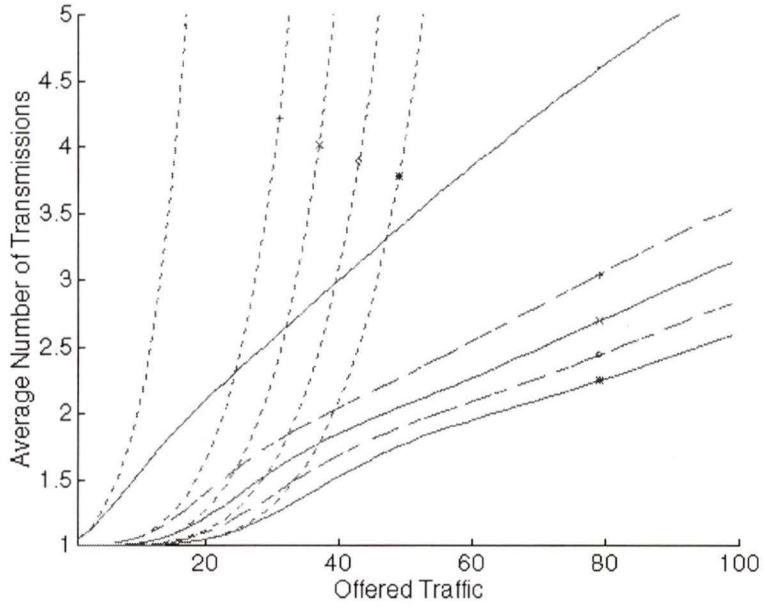

(b)

Figure 4-1. Effects of FEC code rates on the absolute lower bound for normalized throughput (a) and the absolute upper bound for the corresponding average number of transmissions (b).

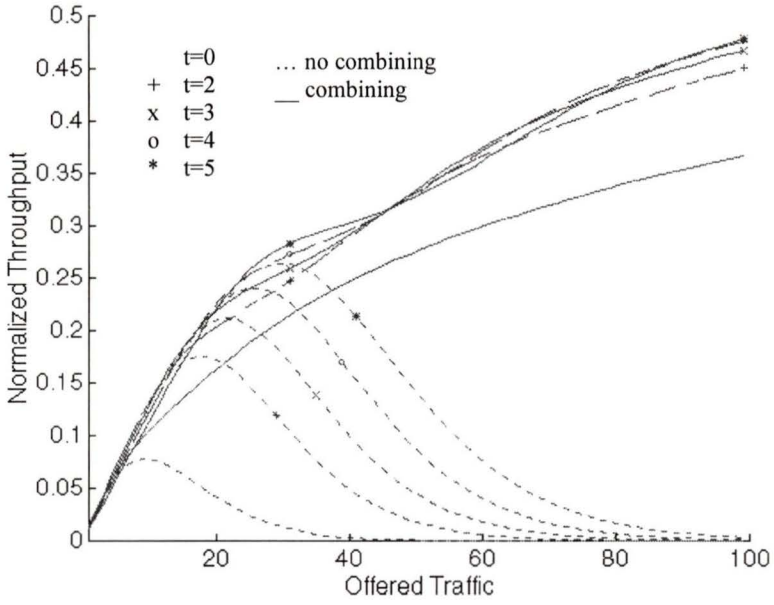

(a)

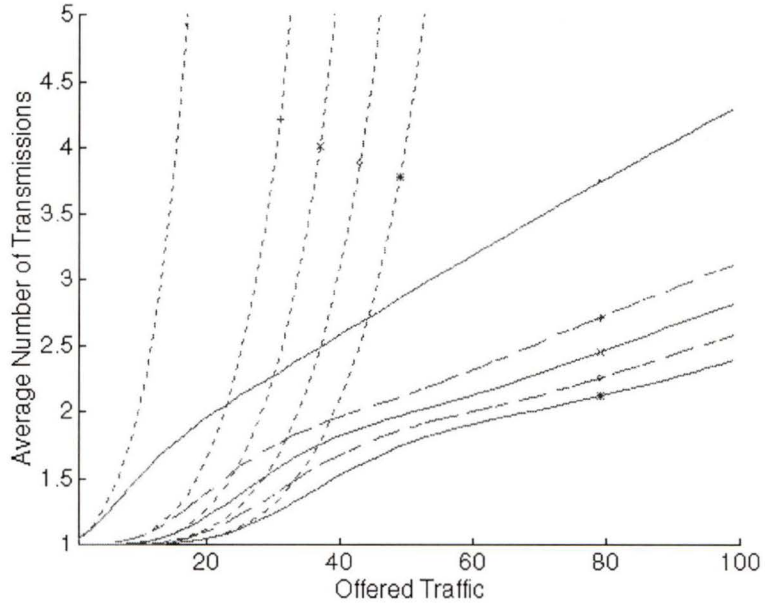

(b)

Figure 4-2. Effects of FEC code rates on the absolute upper bound for normalized throughput (a) and the absolute lower bound for the corresponding average number of transmissions (b).

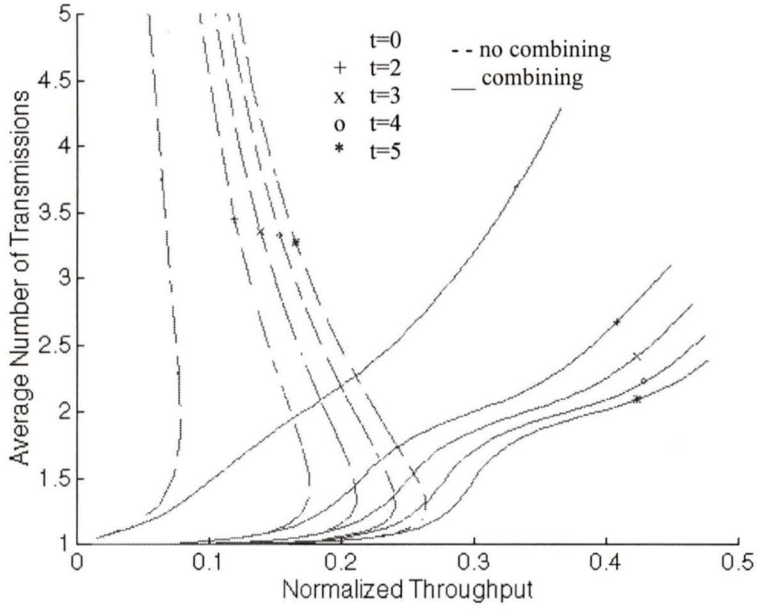

Figure 4-3. Delay-throughput analysis for different FEC code rates, with (solid) and without (dotted) diversity combining.

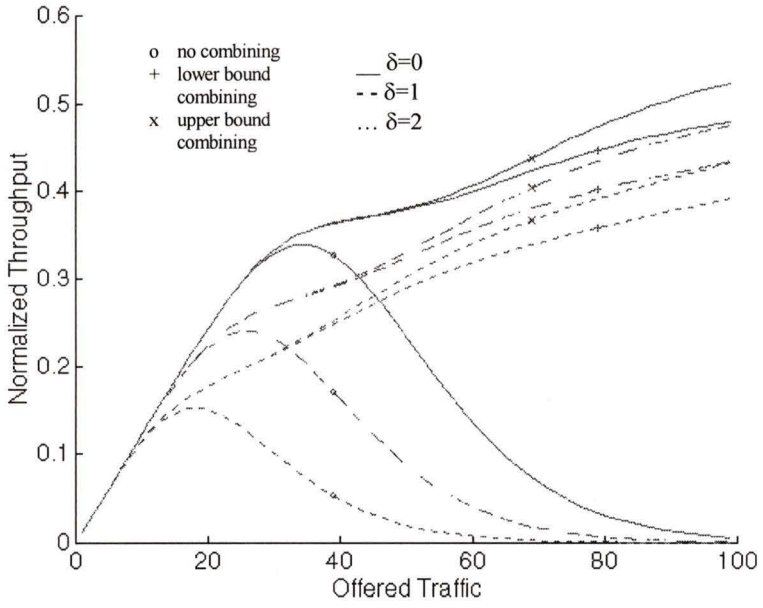

Figure 4-4. Analysis of the effects of MIP decay rate on normalized throughput.

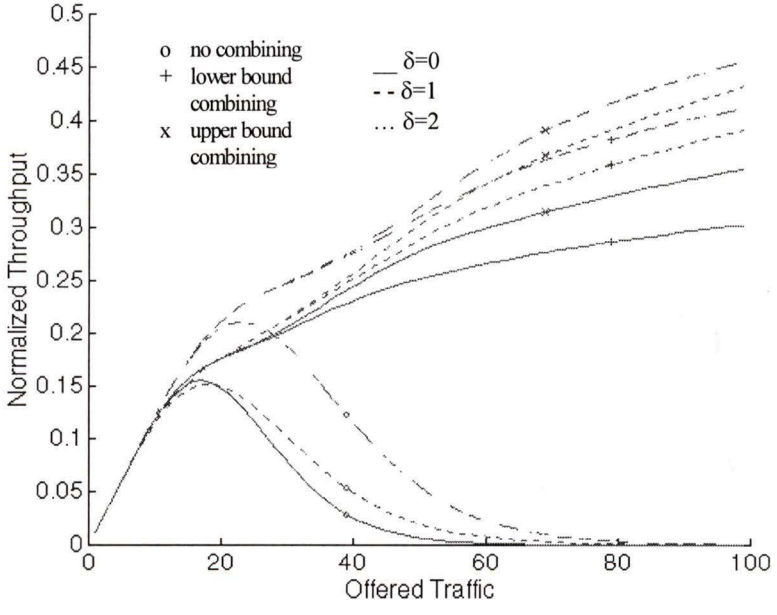

Figure 4-5. Analysis of the effects of reducing the number of fingers on the rake receiver and varying MIP decay rate on normalized throughput.

Chapter 5 Self-Similar Modeled Packet Data with Diversity

5.1 Introduction

In this chapter, throughput analysis of an aggregated self-similar, or fractal, traffic source will be investigated. This type of traffic source has been found to accurately model VBR, ATM traffic. Several studies have concluded that local area and wide area network traffic patterns are very different from the Poisson model [4, 5, 6, 7]. In [20] it is argued that LAN traffic is better modeled by using a self-similar process. In [21] it was found that compressed video traffic closely follows the self-similar model. The traffic generated by self-similar processes are considered to be more bursty than traffic generated by a Poisson process; that is to say that the traffic tends to cluster together more than with a Poisson model.

5.1.1 Correlated Traffic

The correlated nature of traffic can be easily illustrated by some traffic examples. If one looks at the traffic generated by electronic mail (email), it is easy to see that the traffic is much more bursty than Poisson would indicate, and is highly correlated. For a user who is logged in throughout the day, the mail tool checks for new email at specified time intervals. All new email is sent at that time. Furthermore, there is no generation of traffic during the time in between the end of the download and the next check for new

mail request. World Wide Web (WWW) traffic is also very bursty. The usual traffic pattern for the WWW would be a large amount of traffic while the web page is being downloaded and then minimal traffic as the user reads the page. The same can be said for the reading of internet news groups.

The total traffic on the network is also correlated. All networks have some bandwidth limitation. When that limit is approached, the traffic flows can no longer be assumed to be independent. For example, the download rate from an FTP site is heavily dependent on the traffic on that FTP site, and on the traffic on the connection to one's computer.

There are several implications of using self-similar traffic over Poisson traffic to model system performance. The results of Poisson modeling tend to underestimate average packet delay and maximum queue size [7]. In [6] the effect of burstiness on congested networks is investigated. They concluded that, contrary to what Poisson modeling would suggest, linear increases in buffer size do not result in large decreases in packet drop rates.

5.1.2 Aggregated Traffic

Aggregated traffic can be used instead of summing individual independent traffic sources. The first advantage of aggregated traffic is that it is much faster to generate a single traffic source, rather than generate many individual sources. The second advantage is that aggregated traffic is more accurate in a fixed bandwidth situation. Aggregated traffic is more accurate in two ways: The first advantage is that individual traffic sources are not usually independent. For example, when using the WWW, if the network is busy, the download rate is severely impaired. Therefore, other traffic on the

network affects the traffic of the new users. The second advantage is that when modeling individual traffic sources, it is difficult to predict the individual traffic sources to simulate a "real" traffic situation. Although it is possible to trace the generation of packets from individual applications and produce a distribution to model it, one can not account for the changing number of applications or the variations of load from each of the individual users.

5.2 System Description

5.2.1 Generation of Self-Similar Traffic

There are many ways to produce fractional Brownian motion (fBm) and fractional Brownian noise (fBn). These include: Fourier transform, Displacement Process, Pareto distribution, Markov process, and Random Midpoint Displacement methods. The random displacement method (RDM) will be described in depth, as it is the algorithm used in this dissertation. The RDM produces fBm. The output of the RDM is produced by summing up properly scaled Gaussian random numbers in a recursive manner. This can be seen in the following set of iterations in the interval from 0 to 1:

Initialization: $x[0] = 0$

Initialization: $x[1] = R_1$

Iteration 1: $x\left[\frac{1}{2}\right] = \frac{x[0]+x[1]}{2} + hR_2$

Iteration 2: $x\left[\frac{1}{4}\right] = \frac{x[0]+x\left[\frac{1}{2}\right]}{2} + h^2 R_3$

Iteration 2: $x\left[\frac{3}{4}\right] = \frac{x\left[\frac{1}{2}\right]+x[1]}{2} + h^3 R_4$

Iteration 3: $x\left[\frac{1}{8}\right] = \frac{x\left[\frac{1}{2}\right]+x[1]}{2} + h^3 R_5$

Iteration 3: $x\left[\frac{3}{8}\right] = \frac{x\left[\frac{1}{4}\right]+x\left[\frac{1}{2}\right]}{2} + h^3 R_6$

Iteration 3: $x\left[\frac{5}{8}\right]=\frac{x\left[\frac{1}{2}\right]+x\left[\frac{3}{4}\right]}{2}+h^3R_7$

Iteration 3: $x\left[\frac{7}{8}\right]=\frac{x\left[\frac{3}{4}\right]+x[1]}{2}+h^3R_8$

…,

where R_i are normal distributed random numbers. The h factor is a scaling factor related to the Hurst parameter H:

$$h=1/2^H \quad 0<H<1. \tag{5-1}$$

The Hurst parameter has been experimentally found for several types of ATM VBR traffic. Most estimates put the value at around 0.8 [21, 22].

The recursive nature of the RDM can be described as follows: the values of the samples at the two ends of the interval under investigation are initialized to zero and a Gaussian random number respectively. For each iteration, the size of the interval is cut in half. The value of the sample at the half way point is set to the average of the values at the ends of the interval, plus a scaling factor times a Gaussian random number. To generate fBn, the difference between two successive samples is taken.

5.3 Simulation Method

Since there is currently no known closed form mathematical method to model self-similar traffic, simulation must be used to calculate any desired results. Because the traffic is the only portion which has to be simulated, a semi-analytical approach may be adopted for the simulation. The calculation of the packet error probability with combining is performed analytically.

For the results presented here, the following method was used to perform the simulation. First, the self-similar traffic was generated, as described in section 5.2.1, using a Hurst parameter of 0.8. One thousand transmission time slots were simulated for

each value of the average offered traffic. For the results presented in this chapter, the offered traffic ranges from 1 to 100. The generated traffic represents the original traffic for the (s=1,2,…,1000) time slots. The original traffic, $X=(x_s : s=1, 2, 3, \ldots, 1000)$, for each slot, is defined as the traffic that is being sent for the first time. The retransmission traffic, $R_s=(\Sigma r_I(s) : i=1, 2, 3, \ldots)$, is the total number of retransmission packets generated in time slot s, where i represents the number of times the packets have been retransmitted. The total traffic, $W=(w_s : s=1, 2, 3, \ldots, 1000)$, is defined as the original traffic plus the sum of the retransmission traffic for that time slot.

$$w_s = x_s + \sum_{i=1}^{\infty} r_i(s-1). \tag{5-2}$$

$$\begin{aligned} r_i(s) &= r_{i-1}(s-1)Pb_i(w_s) \qquad i>1 \\ r_1(s) &= x_{s-1}Pb_1(w_s) \qquad i=1\text{'} \end{aligned} \tag{5-3}$$

where $Pb_i(w_s)$ is the probability of packet error with w_s packets being sent at that time and ith order diversity. The channel model is the same as described in section 4.1.2 and the packet generation is explained in section 4.1.1. Therefore, $Pb_i(w_s)$ can be defined as,

$$Pb_i(w_s) = 1 - \sum_{x=0}^{t} \binom{N_p}{x} P_i(m+1)^x \left[1 - P_i(m+1)\right]^{N_p - x} \tag{5-4}$$

where P_i is defined in (4-8) and t is the error correction capability.

So, in (5-3) the number of packets to be transmitted for the ith time is calculated for time slot t. In time slot t, the number of packets to be transmitted for the ith time is equal to the number of packets to be transmitted for the (i-1)th time in the previous (t-1)

time slot, multipled by the probability that those packets were in error. Retransmissions occur in the next available time slot.

5.4 Numerical Results

For all of the work presented in this chapter, the processing gain is set to 63 (N=63), the maximum number of resolvable multipaths is equal to 5 (L=5), and the average received SNR of the first arriving path, in the absence of multi-user and self-interference, is set to 15dB ($E[\beta_1^2]E_b/N_o$ = 15dB). The forward error correction used (FEC) in all of the simulations is a 127 bit long BCH code. These are the same codes used in the previous chapter and are shown in Table 4-1.

The block error rate is calculated from the simulated data and is used to find the average number of transmissions, R_{av},. Since the results for (5-4) are only available for integer numbers of users, the value from (5-2) were rounded up or down for the purposes of simulation. If the traffic level was rounded down, the results would be more optimistic than the actual value and the opposite would be true if the traffic level was rounded up. Thus, the results of (5-2) being rounded down can be considered an upper bound and the results of (5-2) being rounded up can be considered a lower bound.

In order for us to compare with other systems, the results must be normalized to the channel utilization efficiency. The throughput results presented in this chapter are shown for normalized throughput η,

$$\eta = \frac{\chi k}{R_{av} N n}, \tag{5-5}$$

where R_{av} is the average number of transmissions for a packet, k/n is coding rate, N is the processing gain, and χ is the average numbered of packets generated during the time slot. The average number of transmissions can be calculated from the following series:

$$R_{av} = 1 + P_b + P_b{}^2 + P_b{}^3 + \ldots, \tag{5-6}$$

where P_b is the average packet error probability. Since $P_b \leq 1$, the geometric series can be simplified to

$$R_{av} = \frac{1}{1 - P_b}. \tag{5-7}$$

In Figure 5-1, the difference between the upper and lower bound can be seen. The gap between the upper and lower bound is very small in the stable regions of the graph. The system for the combining case becomes very erratic and difficult to simulate as the system becomes unstable. So, in the unstable region the results show an approximation of the results, rather than the actual values. The system could be made much more stable if a random back-off algorithm was used. A random back-off algorithm was not used in these results because the effect of the traffic alone was the desired investigation. The results for the no combining case follow the actual values much more closely. For all other plots, only the lower bound will be shown.

In Figure 5-2, the normalized throughput for Poisson and self-similar traffic is compared. The results for the Poisson traffic model used in the previous chapter employed a random back-off algorithm. The back-off algorithm improves the throughput of the system when multiple retransmissions are required, so that as the traffic level increases, the throughput of the Poisson modeled traffic will be higher than the self-similar model. This is the effect of the back-off algorithm and not the traffic model. The

area of interest is the portion of the graph below the cross over point of about an offered traffic of 40 for t=4. Below that point, and below the point where the back-off algorithm has any affect, the self similar traffic has a higher throughput than the Poisson traffic. The back off had no effect at that point because the average number of transmissions had not crossed two transmissions by that point. This can be seen in Figure 5-5.

Figure 5-3 and Figure 5-4 show the effect of the error correction coding. In Figure 5-3, as the amount of offered traffic increases, the benefits of the error correction capability outweigh the added number of redundancy bits. With lower amounts of offered traffic, the channel conditions are more favourable, and the extra redundancy bits are not required. If the amount of offered traffic is unknown, a compromise must be made between the performance at lower traffic levels and the performance at higher traffic levels.

Figure 5-5 shows the average number of transmissions required versus the amount of offered traffic. The average amount of delay before the packet arrives can be compared against the amount of offered traffic. Another way of looking at the reliability of the packets is the to examine the average packet error probability. This is shown in Figure 5-8.

In Figure 5-6, the effect of different MIPs is investigated. Just as in chapter 4, the highest normalized throughput is achieved with a flat MIP (δ=0). The amount of power capture is the highest versus the decaying MIPs. With the power equally spread over all of the branches, the amount of improvement from diversity is maximized. There is significant reduction in power captured for decaying MIPs. This results in a reduction in

throughput. As the MIP decay rate increases, each subsequent copy of the transmission is weaker, and therefore less reliable. Thus, the diversity gains are reduced.

We can see the same trend in Figure 5-7 and Figure 5-6 that we saw in the previous chapter. With Figure 5-7, there are a reduced number of multipaths being passed to the MRC (M=3). For the δ=0 case, this is a 40% reduction in power captured. This translates into the reduced performance. The reduction in the number of multipaths being passed to the MRC has much less effect on more heavily decayed MIP situations. For that reason, the difference between δ=2 case in Figure 5-6 and in Figure 5-7 is minimal.

5.5 Conclusions

The performance of a wireless packet data system with self-similar VBR traffic with and without packet combining has been presented. The combining is performed at the bit level using MRC. For delay sensitive applications, the use of packet combining can greatly reduce the number of required transmissions to decode a correct packet. The differences between self-similar and Poisson traffic were also investigated. It was found the throughput of the self-similar traffic was higher than that of the Poisson traffic. This can be attributed to the fact that the self-similar traffic is more bursty than that of the Poisson traffic. With differing MIPs, it was found that the normalized throughput was higher for flatter multipath profiles (smaller δ), as was found in the Poisson traffic case.

The effect of reducing the number of fingers on the rake receiver was also investigated. With the reduced number of paths captured, flatter multipath profiles suffered from the reduction in power captured. The effect of reducing the number of fingers as the MIP decay rate is increased (larger δ) is minimal. This means that for a

channel with a large MIP decay rate, the advantage of having many fingers on the rake receiver is minimal.

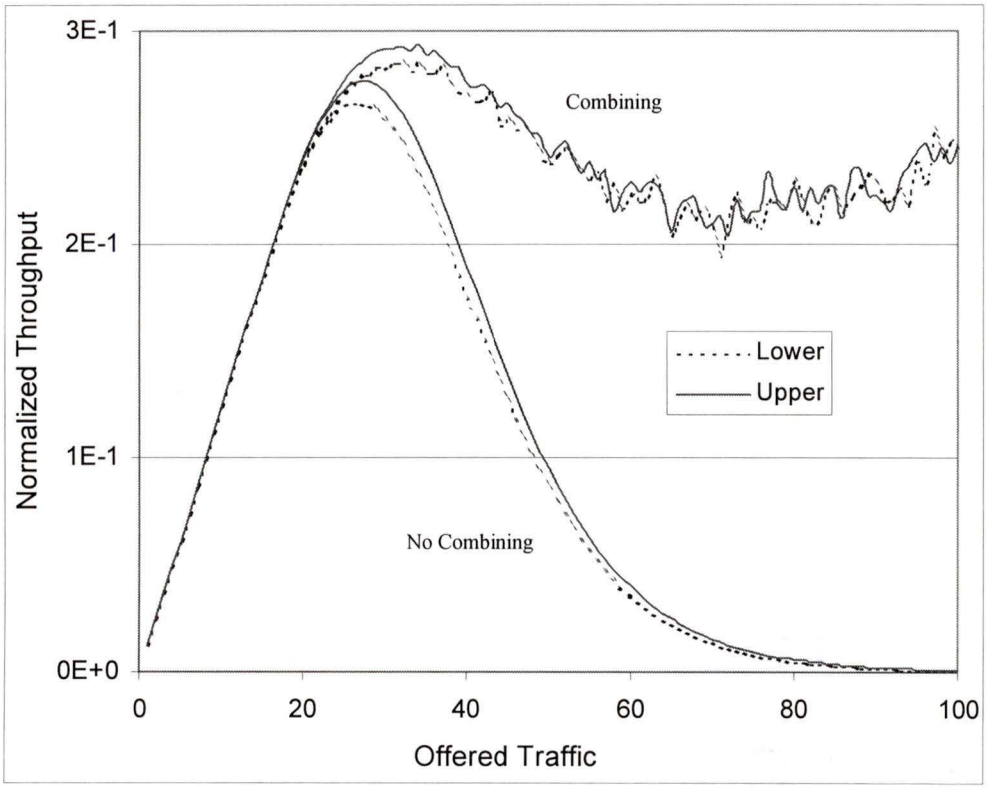

Figure 5-1. Upper and Lower bound for combining and no combining.

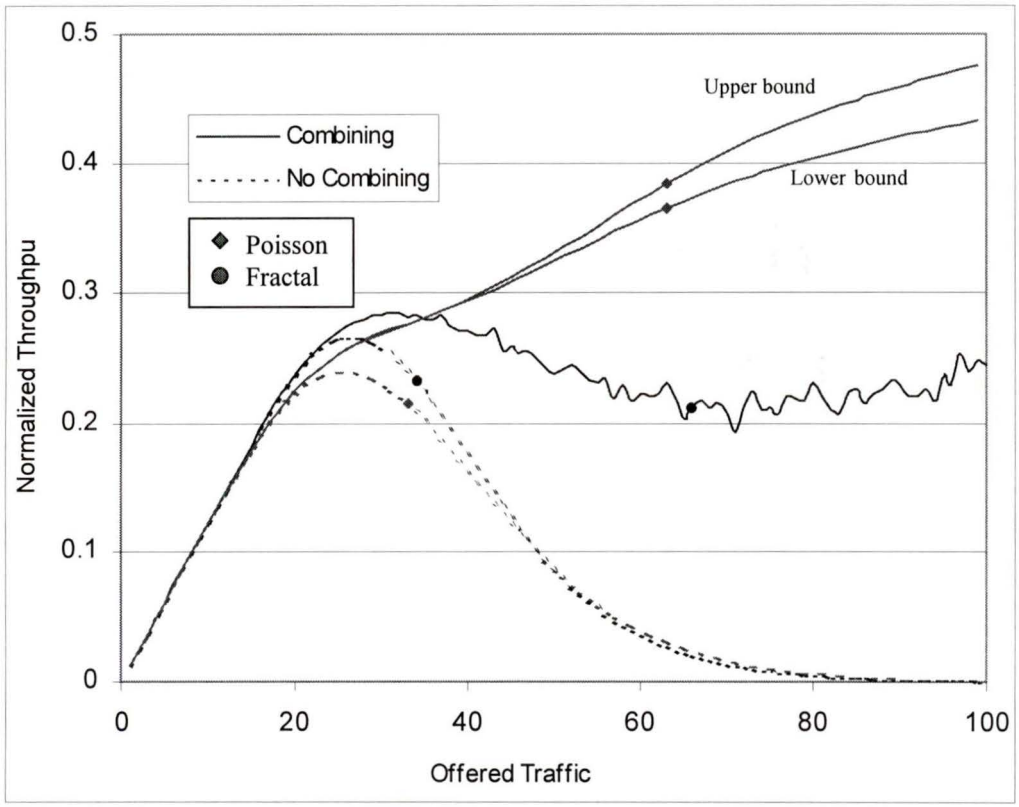

Figure 5-2. Upper and lower bound of Poisson traffic versus lower bound self-similar traffic with and without combining. A (127,99,4) BCH code was used for FEC.

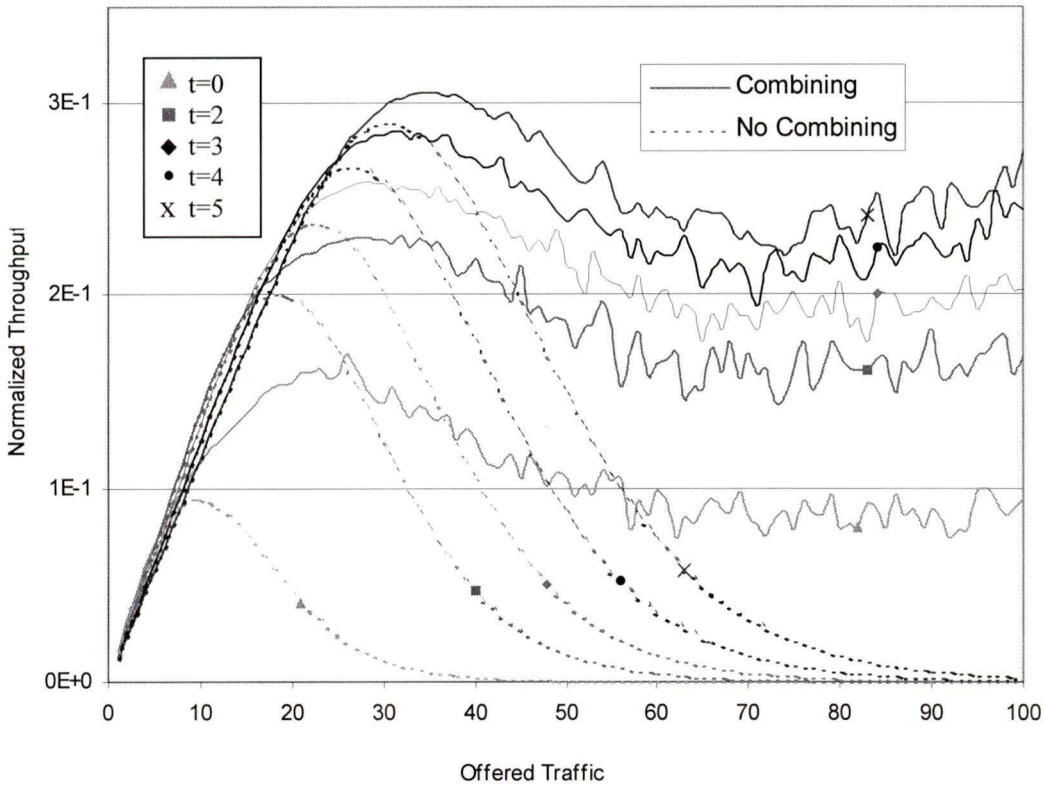

Figure 5-3. Effect of error correction capabilities for combining and no combining. (127,92,5), (127,99,4), (127,106,3), (127,113,2) and (127, 127,0) BCH codes were used for FEC.

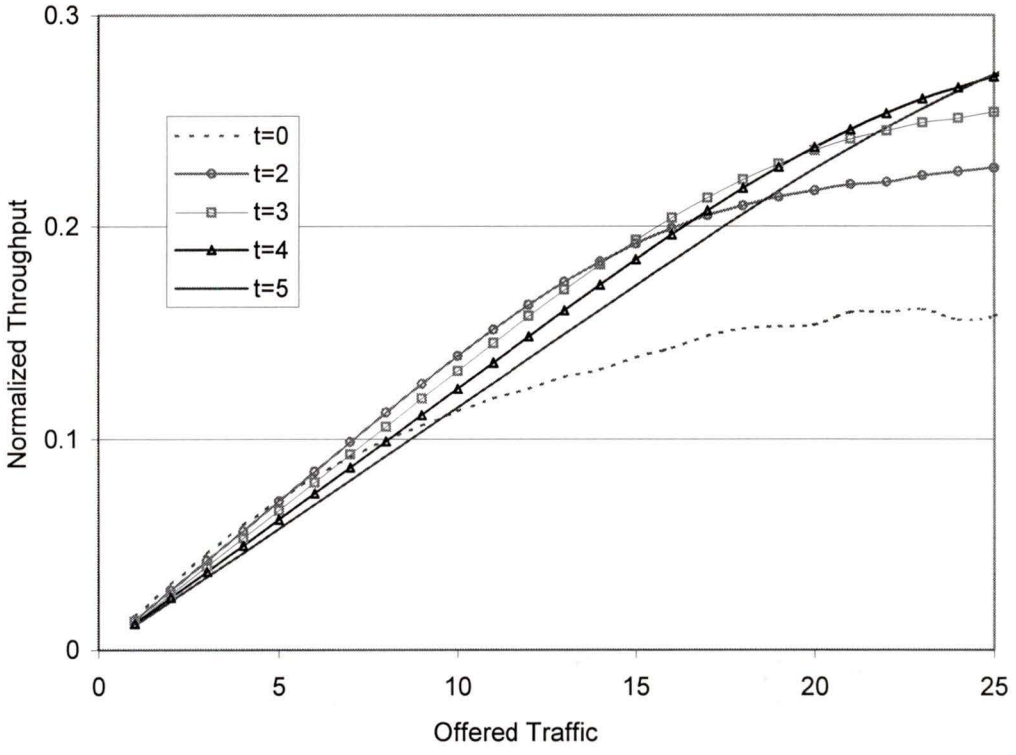

Figure 5-4. Expanded view of Figure 4-3, from an offered traffic of 0 to 25.

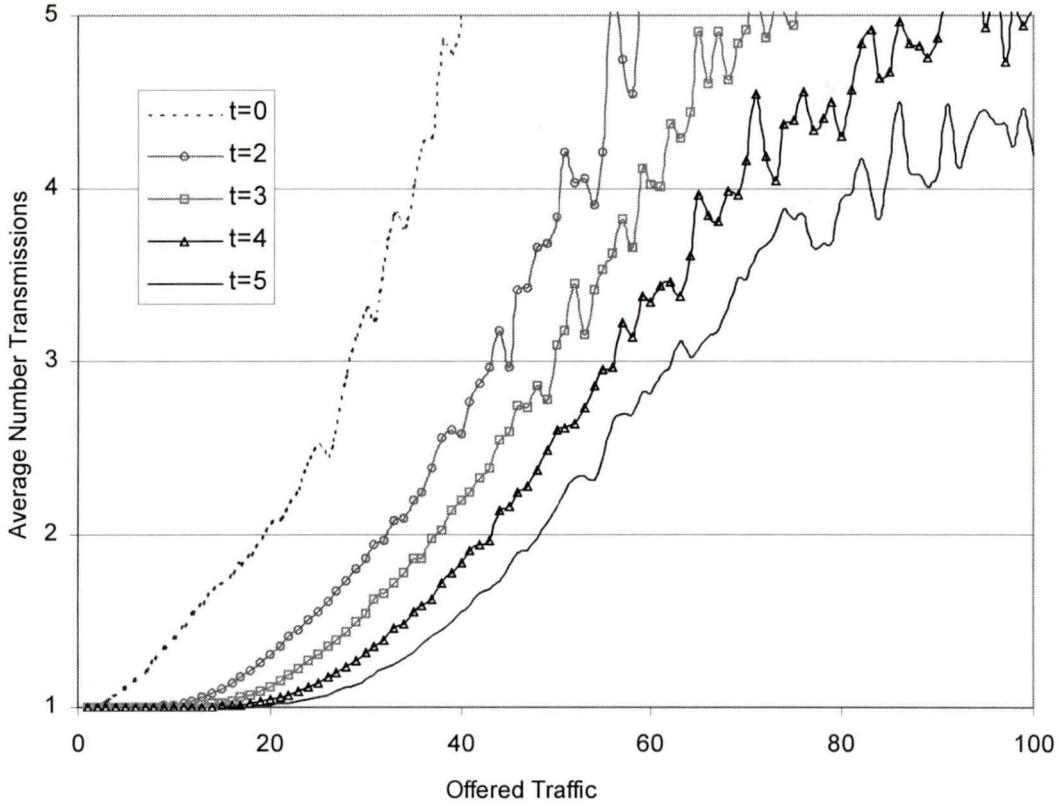

Figure 5-5. Average number transmissions for different error correction capabilities. (127,92,5), (127,99,4), (127,106,3), (127,113,2) and (127, 127,0) BCH codes were used for FEC.

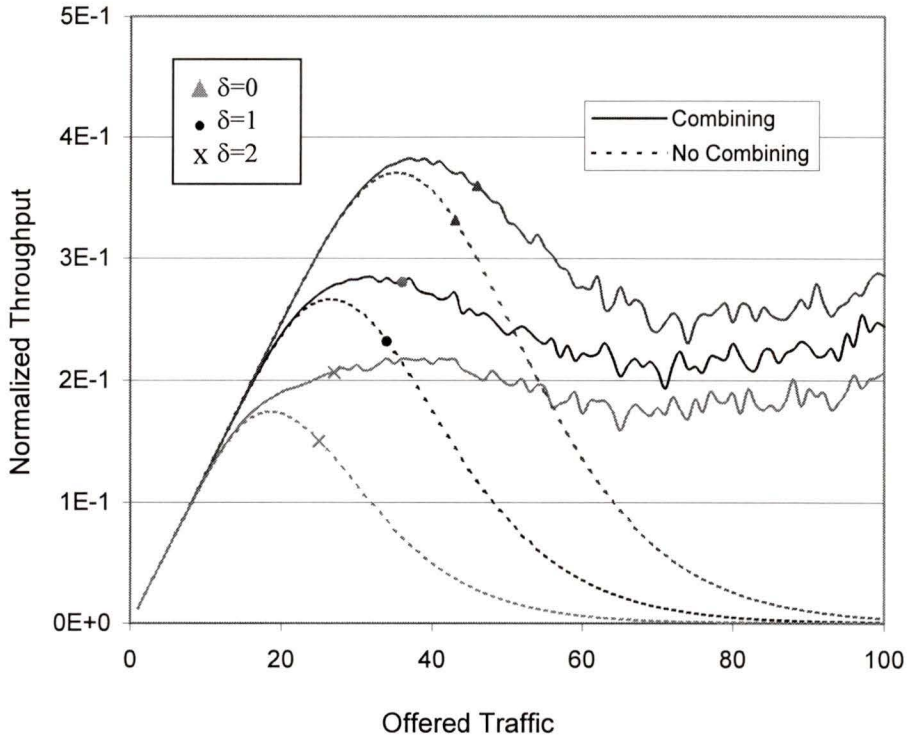

Figure 5-6. Three different MIPs compared with and without combining (δ=0, δ=1, and δ=2).

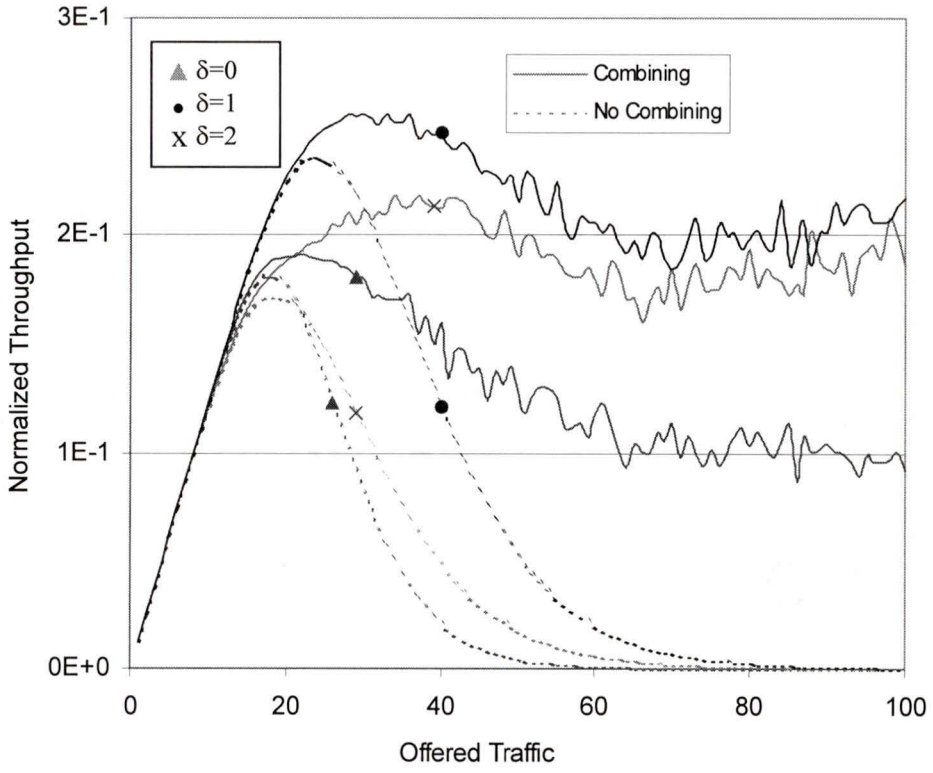

Figure 5-7. Three different MIPs (δ=0, δ=1, and δ=2) using a reduced complexity rake receiver (M=3) are compared with and without combining.

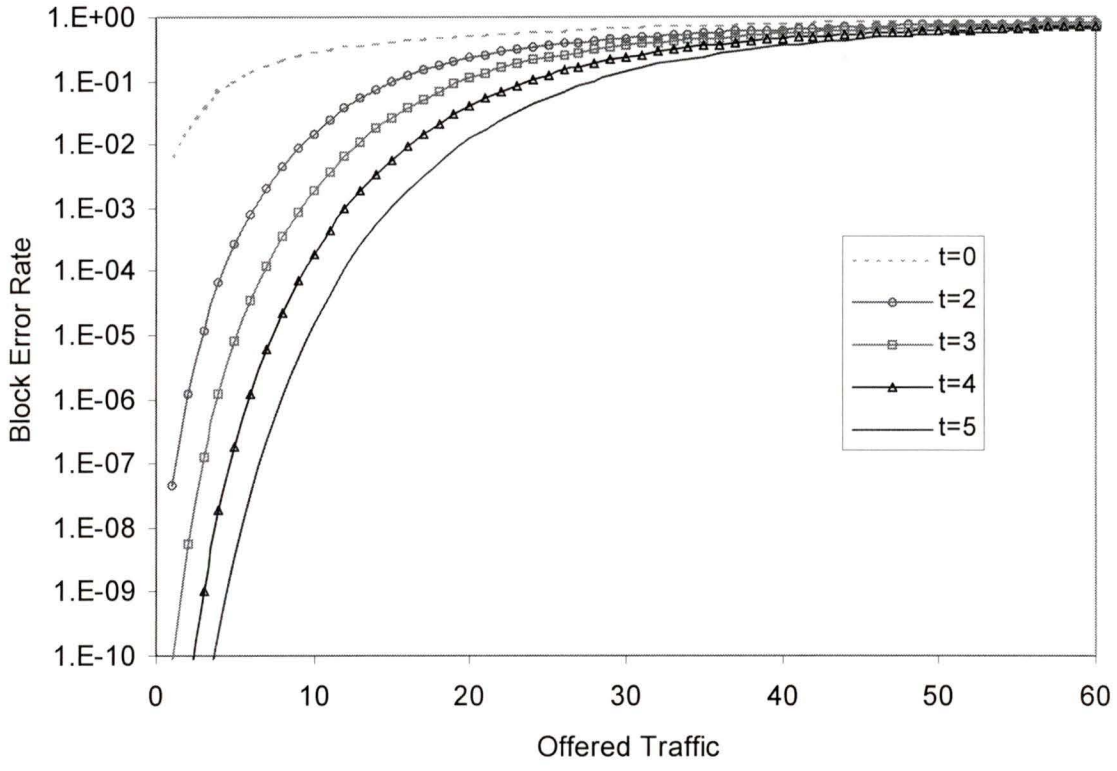

Figure 5-8. Lower bound block error rate comparison using self-similar traffic. (127,92,5), (127,99,4), (127,106,3), (127,113,2) and (127, 127,0) BCH codes were used for FEC.

Chapter 6 Conclusions

This dissertation examined the performance enhancement of using diversity in DS-CDMA networks. Since spectrum is limited, maximizing channel utilization is very important. In order to improve channel utilization, additional complexity must be used somewhere in the system. It is important to weigh the trade-offs between the performance gained and additional complexity. In the previous chapters, the performance of two different diversity techniques has been examined. The amount of degradation with a lower complexity receiver is also examined in each chapter.

In Chapter 3, two variations of rake receivers are compared to the optimum MRC receiver. The effect of different fading environments and different MIPs was also investigated. The pre-selection selection MRC was found to outperform the reduced tap MRC, and performs closely to the optimum MRC in most channel situations. When the channel MIP was more steeply decaying, the performance gap between each of the methods was very small. It was also important to note that in practical systems there are losses that are a result of combining, so the addition of more diversity branches introduces a certain amount of loss. Therefore, if the channel was known to follow a steeply decaying MIP, a reduced complexity, finite tap MRC can be employed with very limited performance degradation. The small drop in performance was due to the very small incremental gains in power capture by adding more branches.

In chapter 4, the performance increase of using time diversity in a wireless packet data system was analyzed. The traffic was modeled as a Poisson random process.

Analytical expressions calculating the average number of transmissions and the normalized throughput were also presented. From the numerical results, the use of packet combining greatly enhances the normalized throughput over a traditional non-combining system. Forward error correction can further increase the reliability of the transmissions, overcoming the increase in overhead of the use of redundancy bits. Investigation of different MIPs show that the normalized throughput was higher for flatter MIPs. The effects of using a finite tap rake receiver are the same as in chapter 3: channels with more steeply decaying MIPs experience minimal degradation in performance by using a reduced complexity receiver.

In chapter 5, the effect of modeling traffic using a self-similar model is investigated on a packet diversity system. This system was compared against the results of the Poisson traffic system that was discussed in chapter 4. As in chapter 4, the use of packet combining greatly reduces the number of required transmissions to decode a correct packet. A self-similar modeled system had a higher normalized throughput than that of the Poisson modeled system. This difference is due to the more bursty nature of the self-similar modeled traffic as compared to that of the Poisson modeled traffic. The effects of FEC are similar to those found in chapter 4. The use of FEC increased the normalized throughput of the system as the channel conditions deteriorated. The use of a finite tap receiver also had the same effect as in chapter 4. This allows the use of a reduced complexity receiver with nominal loss in normalized throughput.

6.1 Recommendations for Further Work

In each of the chapters, there are aspects of the system that could be further explored. Some of the investigations that are yet to be performed are described in the following paragraphs:

1. In chapter 3, the system is investigated with the assumption that the power is constant over all MIPs. The performance of the system could be found with the MIP calculated in the same way as in chapters 4 and 5.
2. In chapter 4, the performance of each of the bounds can be examined by the use of simulation.
3. In chapter 5, the results would be directly comparable with those in chapter 4 if the system employed a random exponential back-off algorithm.
4. Examination of some of the heavy tailed distributions for analytical modeling of self-similar traffic would allow for the removal of the need for simulation results.

References

[1] M. Jerome, "Air War," BYTE, Vol. 22, No. 8, pp. 93-99, August 1997.

[2] T. Eng, N. Kong and L. B. Milstein, "Comparison of Diversity Combining Techniques for Rayleigh Fading Channels," *IEEE Trans. Commun.,* Vol. 44, pp. 1117-1129, September 1996.

[3] M. Pursley, "The Role of Spread Spectrum in Packet Radio Networks," *Proceedings of the IEEE*, Vol. 75, No. 1, January 1987, pp 116-134.

[4] R. Jain and S. Routhier, "Packet Trains – Measurements and a New Model for Computer Network Traffic," *IEEE JSAC*, Vol. 4 number 6, pp 986-995, September , 1986.

[5] R. Gussela, "A Measurement Study of Diskless Workstation Traffic on an Ethernet," *IEEE Transactions on Communications*, Vol. 38 No. 9, pp 1557-1568, September, 1990.

[6] H. Fowler and W. Leland, "Local Area Network Traffic Characteristics, with Implications for Broadband Network Congestion Management," *IEEE JSAC*, Vol. 9 No 7, pp 1139-1149, September 1990.

[7] V. Paxson and S. Floyd, "Wide-Area Traffic: The Failure of Poisson Modeling," *ACM SIGCOMM 94*, pp 257-267, August 1994.

[8] J. Proakis, *Digital Communications 3rd Ed.*, New York: McGraw-Hill, Inc., 1995.

[9] M. Nakagami, "The m-Distribution – A general Formula of Intensity Distribution of Rapid Fading," *Statistical Methods of Radio Wave Propagation*, Pergamon Press, New York, 1960.

[10] William C. Y. Lee, *Mobile Communications Design Fundamentals 2nd Ed.*, New York: John Wiley and Sons, 1993.

[11] D. Davis and S. Gronemeyer, "Performance of slotted ALOHA random acces with delay capture and randomized time of arrival," IEEE Transactions on Communications, Vol. Cpm-28, pp. 703-710, May 1980.

[12] D. Raychaudhuri, "ATM Based Transport Architecture for Multiservices Wireless Personal Communication Networks," *IEEE ICC 94*, pp 559-565.

[13] G. L. Stuber, *Principles of Mobile Communication*, Kluwer Academic Publishers, Boston, 1996.

[14] A. Annamalai and V. K. Bhargava, "Evaluation of a Low-Complexity Rake Receiver for the Narrowband-CDMA Indoor Wireless Channels," *Proc. International Wireless and Telecommunications Symposium*, Shah Alam, May 14-16, 1997.

[15] T. Eng and L. B. Milstein, "Comparison of Hybrid FDMA/CDMA Systems in Frequency Selective Rayleigh Fading," *IEEE J. Select. Areas Commun.*, Vol. 12, pp. 938-951, June 1994.

[16] Q. T. Zhang, "Outage Probability in Cellular Mobile Radio Due to Nakagami Signal and Interferers with Arbitrary Parameters," *IEEE Trans. Vehic. Technology*, Vol. 45, pp. 364-372, May 1996.

[17] D. Raychaudhuri, "Performance Analysis of Random Acces Packet-Switched Code Division Multiple Access Systems," IEEE Transactions Communications, Vol 29, pp. 895-901, June 1981.

[18] S. Lin and D. Costello, Error Control Coding Fundamentals and Applications, Prentice-Hall, New Jersey.

[19] A. Annamalai, Issues in DS-CDMA Integrated Wireless Access Networks, M. A. Sc Thesis, University of Victoria, BC, Canada, 1997.

[20] W. Leland, et al., "On the Self-Similar Nature of Ethernet Traffic," *IEEE/ACM Transactions on Networking*, pp 1-15, February 1994.

[21] M. Garrett and W. Willinger, "Analysis, Modeling and Generation of Self-Similar VBR Video Traffic," *ACM SIGCOMM 94*, pp 269-280, August 1994.

[22] P. Droz and J. Y. Le Boudec, "A High-Speed Self-similar ATM VBR Traffic Generator," *Proc. IEEE Globecom 96*, pp 586-590.

APPENDIX A

If α_k is characterized statistically by the Nakagami-m distribution, the random variable $\gamma_k = \alpha_k^2 \mathscr{E}_b / N_o$, has the probability density function,

$$f_{\gamma_k}(y) = \frac{m^m}{\Gamma(m)\bar{\gamma}_k{}^m} y^{m-1} \exp\left(\frac{-my}{\bar{\gamma}_k}\right) \tag{A.1}$$

where $\bar{\gamma}_k = E(\alpha_k^2)\mathscr{E}_b / N_o$. Maximum-ratio combining is known to be optimum in the sense that it yields the best statistical reduction of fading in any linear diversity combiner. In this technique, the M diversity branches are first co-phased and then weighted in proportion to their signal level before summing. The output of the maximum-ratio combiner can be expressed as a single decision variable in the form [1],

$$U = \mathrm{Re}\left(2\mathscr{E}_b \sum_{k=1}^{M} \alpha_k{}^2 + \sum_{k=1}^{M} \alpha_k N_k\right) = 2\mathscr{E}_b \sum_{k=1}^{M} \alpha_k{}^2 + \sum_{k=1}^{M} \alpha_k N_k \tag{A-2}$$

For a fixed set of $\{\alpha_k\}$the decision variable U is Gausssian with mean $E(U) = 2\mathscr{E}_b \sum_{k=1}^{M} \alpha_k{}^2$

and variance. $\sigma_U{}^2 = 2\mathscr{E}_b N_o \sum_{k=1}^{M} \alpha_k{}^2$. For these values of the mean and variance, the probability that U is less than zero is simply,

$$P(\gamma_b) = Q(\sqrt{2\gamma_b}) \tag{A-3}$$

where the SNR per bit, γ_b is given as

$$\gamma_b = \frac{\mathscr{E}_b}{N_o} \sum_{k=1}^{M} \alpha_k{}^2 = \sum_{k=1}^{M} \gamma_k \tag{A-4}$$

where γ_k is the instantaneous SNR on the *k*th diversity branch. If we assume that the fading at each branch to be mutually statistically independent, then the characteristic

function for the sum of γ_k, k=1,2,…,M, is simply the product of their individual characteristic functions, i.e.,

$$\psi_{\gamma_{mrc}}(jv) = \prod_{k=1}^{M} \frac{1}{\left(1 - jv\frac{\bar{\gamma}_k}{m}\right)^m} = \sum_{k=1}^{M}\sum_{q=1}^{m} \frac{A_{kq}}{\left(1 - jv\frac{\bar{\gamma}_k}{m}\right)^q} \tag{A-5}$$

where A_{kq} is given by

$$A_{kq} = \frac{(-m)^{m-q}}{(m-q)!\,\bar{\gamma}_k{}^{m-q}} \frac{d^{m-q}}{ds^{m-q}} \left\{ \prod_{\substack{i=1 \\ i\neq k}}^{M} \left[1 - \frac{s\bar{\gamma}_i}{m}\right]^{-m} \right\}\Bigg|_{s=\frac{m}{\bar{\gamma}_k}} \tag{A-6}$$

The inverse Fourier transform of the characteristic function gives the probability density function of γ_{mrc} in the form,

$$f_{\gamma_{mrc}}(x) = \sum_{k=1}^{M}\sum_{q=1}^{m} A_{kq} \frac{m^q x^{q-1}}{\Gamma(q)\bar{\gamma}_k{}^q} \exp\left(\frac{-mx}{\bar{\gamma}_k}\right). \tag{A-7}$$

Therefore, the average bit error probability is given by,

$$P_b = \sum_{k=1}^{M}\sum_{q=1}^{m} A_{kq} \int_0^{\infty} Q\left(\sqrt{2x}\right) \frac{m^q x^{q-1}}{\Gamma(q)\bar{\gamma}_k{}^q} \exp\left(\frac{-mx}{\bar{\gamma}_k}\right) dx. \tag{A-8}$$

The definite integral in (A-8) has a known closed-form solution (e.g., [15]),

$$\int_0^{\infty} Q\left(\sqrt{2x}\right) \frac{m^q x^{q-1}}{\Gamma(q)\bar{\gamma}_k{}^q} \exp\left(\frac{-mx}{\bar{\gamma}_k}\right) dx$$

$$= \frac{(2q-1)!\,m^q\, {}_2F_1\left(q, q+\frac{1}{2}, q+1, -m/\bar{\gamma}_k\right)}{2^{2q}\bar{\gamma}_k{}^q (q-1)!q!} \tag{A-9}$$

$$= \left[\frac{1-\mu_k}{2}\right]^q \sum_{i=0}^{q-1} \binom{q-1+i}{i} \left[\frac{1+\mu_k}{2}\right]^i \tag{A-10}$$

where $\mu_k = \sqrt{\frac{\bar{\gamma}_k}{m+\bar{\gamma}_k}}$ and ${}_2F_1(a,b,c,d)$ is the Gauss hypergeometric function. Therefore, by substituting (A-10) into (A-8), equation (3-4) is readily shown.

VITA

Surname: Wong **Given Names**: Richard Shiu Chung

Place of Birth: Hong Kong

Educational Institutions Attended:

University of Victoria	1990-1997

Degrees Awarded:

Bachelors of Engineering with Distinction	1995

Honours and Awards:

NSERC Post Graduate Scholarship (Doctoral)	1997
UVic President's Graduate Research Scholarship	1997
NSERC Post Graduate Scholarship (Masters)	1996
Advanced Systems Institute of BC GARP scholarship	1996
UVic President's Graduate Research Scholarship	1996
APEGBC Proficiency Prize	1996
MPR TelTech Scholarship	1994
UVic President's Scholarship	1994
Canada Scholarship (renewed)	1994
UVic Faculty Scholarship	1993
NSERC Undergraduate Research Scholarship	1993
The Charles Humphrey Memorial Scholarship	1993
Canada Scholarship (renewed)	1993
UVic President's Scholarship	1992
Woods Trust Scholarship	1992
UVic Faculty Scholarship	1992
Canada Scholarship (renewed)	1992
UVic President's Scholarship	1991
Canada Scholarship (renewed)	1991
Governor General's Bronze Medal	1990
Canada Scholarship	1990
The William Clark Mearns Scholarship	1990
B.C. Provincial Scholarship	1990
UVic Dean of Engineering Entrance Scholarship	1990

Publications:

Journal

A. Annamalai, R. S. C. Wong, and V. K. Bhargava, "Improving the Delay and Throughput Performance of Random Access DS-CDMA Radio Networks with Packets Combining," submitted to *IEEE Transactions on Communications*.

A. Annamalai and R. S. C. Wong, "Diversity Combination of Finite-Tap Statistics on Generalized Fading Channels," submitted to *IEEE Transactions on Communications*.

Refereed Conference

Richard Wong and Vijay K. Bhargava, "Evaluation of Predetection Diversity Techniques for Rake Receivers," *Proceedings of the IEEE Pacific Rim Conference 1997.*

Richard Wong and Vijay K. Bhargava, "Denoising of Low SNR Signals Using Composite Wavelet Threshold Selection," *Proceedings of the IEEE Pacific Rim Conference 1997.*

A. Annamalai, Richard Wong and Vijay K. Bhargava, "Throughput Enhancement of a Slotted DS/CDMA ALOHA with Packet Combining," *Proceedings of the IEEE Pacific Rim Conference 1997.*

PARTIAL COPYRIGHT LICENSE

I hereby grant the right to lend my dissertation to users of the University of Victoria Library, and to make single copies only for such users or in response to a request from the Library of any other university, or similar institution, on its behalf or for one of its users. I further agree that permission for extensive copying of this dissertation for scholarly purposes may be granted by me or a member of the university designated by me. It is understood that copying or publication of this dissertation for financial gain shall not be allowed without my written permission.

Title of Dissertation: ANALYSIS OF DIVERSITY TECHNIQUES FOR IMPROVING THE PERFORMANCE OF DS-CDMA DATA NETWORKS

Author

Richard S. C. Wong
September 1, 1997